Insights from the Unseen - Occlusion in Forest Laser Scanning

Daniel Kükenbrink[a,1,*], Matthias Gassilloud[b,1], Benjamin Brede[c], Aline Bornand[n], Kim Calders[j], Wout Cherlet[j], Markus P Eichhorn[d,e], Julian Frey[i], Charis Moana Gretler[a], Bernhard Höfle[h,g], Teja Kattenborn[b], Lennart Klinger[m], Martin Mokroš[l], Timo P Pitkänen[f], Ninni Saarinen[k], Louise Terryn[j], Hannah Weiser[h,g], Anna Göritz[b]

[a] *Landchange Science, Swiss Federal Institute WSL, Zürcherstrasse 111, Birmensdorf, CH-8903, Switzerland*
[b] *Chair of Sensor-based Geoinformatics (geosense), University of Freiburg, Tennenbacherstr. 4, D-79106, Freiburg, Germany*
[c] *GFZ Helmholtz Centre for Geosciences, Telegrafenberg, Potsdam, 14473, Germany*
[d] *School of Biological, Earth & Environmental Sciences,University College Cork, Distillery Fields, North Mall, Cork, T23 N73K, Ireland*
[e] *Sustainability Institute, University College Cork, Lee Rd, Sunday's Well, Cork, T23 XE10, Ireland*
[f] *Natural Resources Institute Finland (LUKE), Latokartanonkaari 9, Helsinki, FI-00790, Finland*
[g] *3DGeo Research Group, Institute of Geography, Heidelberg University, Im Neuenheimer Feld 368, Heidelberg, 69120, Germany*
[h] *Interdisciplinary Center for Scientific Computing (IWR), Heidelberg University, Im Neuenheimer Feld 205, Heidelberg, 69120, Germany*
[i] *Forest Growth and Dendroecology, University of Freiburg, Tennenbacherstr. 4, Freiburg, 79106, Germany*
[j] *Q-ForestLab, Department of Environment, Faculty of Bioscience Engineering, Ghent University, Belgium, Campus Coupure, Coupure links 653, Ghent, 9000, Belgium*
[k] *School of Forest Sciences, University of Eastern Finland, P.O. Box 111, Joensuu, FI-80101, Finland*
[l] *Department of Geography, University College London, Gower Street, London, WC1E6BT, UK*
[m] *Laboratory of Geo-Information Science and Remote Sensing, Wageningen University, Droevendaalsesteeg 3, Gaia, building number 101, Wageningen, 6708 PB, the Netherlands*
[n] *Forest Resources and Management, Swiss Federal Institute WSL, Zürcherstrasse 111, Birmensdorf, CH-8903, Switzerland*

*Corresponding author: daniel.kuekenbrink@wsl.ch
[1]These authors contributed equally to this work

Abstract

Laser scanning is a powerful tool for assessing the structural complexity of forests and its role in ecosystem processes and functioning. Laser scans are however highly affected by occlusion (where objects block laser pulses), resulting in data gaps within the 3D representation of the forest. Although occlusion is a well-known and frequently discussed challenge for estimating forest structural information from laser scanning data, it is rarely quantified. Here, we describe the concept of occlusion and distinguish different types. We examine the primary causes of occlusion, discuss the role of forest structure, viewpoint arrangement, and laser system properties along with platform-specific challenges. We further present comprehensive strategies to mitigate and recent tools for detecting occlusion in laser scanning acquisitions. Finally, we highlight a broad range of research avenues for occlusion mapping ranging from uncertainty quantification, data completion, and intelligent autonomous laser scanning acquisition. By raising awareness of occlusion and showcasing its methodological and practical implications, this work aims to inspire new advances in the assessment of forest structure through laser scanning.

Keywords: LiDAR, occlusion, point cloud quality, forest structure, raytracing, volume exploration, ULS, MLS, TLS

1. Introduction

Forest structure plays a vital role in ecological processes and ecosystem functioning. It regulates how solar radiation is absorbed, transmitted, and reflected (Kükenbrink et al., 2021), influencing processes related to energy and matter fluxes (Damm et al., 2020; Kesselring et al., 2024), and microclimate (Zellweger et al., 2020). The structure of forests determines habitat availability and heterogeneity, making it a key control for biodiversity (Helbach et al., 2022; Knuff et al., 2020; Heidrich et al., 2020), and it is closely linked to aboveground biomass and carbon storage (Lefsky et al., 2002). Consequently, assessing forest structure is essential for understanding forest dynamics and functioning in the face of climate change and the biodiversity crisis (Ehbrecht et al., 2021; Pan et al., 2013; Pörtner et al., 2021).

Laser scanning (also called Light detection and ranging (LiDAR)) technologies have become an important tool for quantifying forest structure at a high level of detail and accuracy. Laser scanning, which collects spatial information from the reflections of emitted laser beams, can capture the 3D distribution of vegetation components, enabling the assessment of tree crown dimensions, foliage distribution, and 3D complexity (Calders et al., 2020; Ehbrecht et al., 2026; Frey et al., 2025; Liang et al., 2022). By providing such detailed 3D structural information, laser scanning plays a crucial role in addressing pressing research questions related to biodiversity (Toivonen et al., 2023), habitat heterogeneity (Moudrý et al., 2023; Helbach et al., 2022), biomass distribution (Seidel et al., 2011), disturbance impacts (Barrere et al., 2024; Jactel et al., 2017) and facilitates modelling of forest responses to environmental change (Calders et al., 2025).

While laser scanning is frequently used to assess structural properties of forests, the acquired point clouds are rarely critically evaluated regarding their suitability to answer the posed research questions. It is often assumed that the acquired point clouds represent the targeted forest structural parameters in question without quantitative verification. This is less of an issue if accurate reference measurements for forest structural parameters are available (e.g. tree/canopy height, diameter at breast height (DBH), and tree position), as the quality of the point clouds can be assessed through the accuracy of the parameters derived from the point cloud. However, poor representativeness of acquired point clouds may obscure limited reliability of methods when transferring approaches to more complex sites, where reference data might not be available. This problem is even more pronounced for various forest structural parameters for which accurate reference measurements are difficult to obtain (e.g. vegetation density, canopy layering, structural complexity), rendering validation and calibration difficult. Here the assumption of representativeness could easily result in biased conclusions.

Assessing the quality of a point cloud in terms of its suitability is not a trivial task, and so far no robust and generic method for such an assessment exists. Most often, simple point cloud metrics such as point density or minimum distance between neighbouring points are used to indicate the completeness or quality of a point cloud (e.g., Wilkes et al., 2017; Calders et al., 2020). Point density metrics offer only a limited perspective on a point cloud's ability to capture structural complexity though, indicating point spacing but not the actual forest volume represented.

Since forest volume comprises both vegetation and gaps, understanding point cloud completeness or representativeness requires analysing not just the captured vegetation but also the spaces between objects. Gaps in the acquired forest point clouds are caused by either a) true empty space, b) missed objects (which lie between laser beams, or which are hit but their reflected energy is below the detection threshold of the laser scanning device), or c) occlusion (where an object is obstructing the beam from further propagation). While the first two causes are either properties of the forest structure itself, the scan design or the scanning device, occlusion is caused by the interaction between the scan and the scene being measured. Occlusion can prevent laser scanning from capturing the full 3D structure, substantially reducing the representativeness of the resulting point cloud and hence limiting the capacity of the acquired point cloud to capture forest structural parameters.

So far only a few studies have explicitly addressed the issue of occlusion, with a focus on assessing the coverage and completeness of the acquired point clouds (e.g. Brede et al., 2022; Gassilloud et al., 2025; Kükenbrink et al., 2017; Morsdorf et al., 2018). A few studies also investigated the effect of occlusion on the derivation of specific structural metrics (e.g. Ehbrecht et al., 2026; Schneider et al., 2019; Yun et al., 2019). Most recent studies using laser scanning data for forest attribute estimation rely on methodological approaches to reduce occlusion through regular scan position distribution for terrestrial laser scanning (TLS) campaigns (e.g. Wilkes et al., 2017) or fixed overlaps between flight lines for unoccupied aerial vehicle laser scanning (ULS) acquisitions (e.g. Gassilloud et al., 2025) without accounting for variation in forest structure. The impact of occlusion on the estimation of forest structural metrics is typically not considered at all. There is therefore a critical gap in effective and scalable methods to map and account for occlusion in the estimation of forest structural metrics. By systematically implementing occlusion mapping in forest structural assessments and accounting for its effects on derived metrics, the robustness of laser scanning–based analyses can be greatly enhanced. This, in turn, would substantially improve the ability to quantify structural changes from repeated acquisitions and strengthen forest monitoring capabilities.

Here we provide a perspective on the benefits of occlusion mapping as a tool to assess point cloud completeness and suitability. We define and describe different types of occlusion in acquired point cloud data and discuss impacts of occlusion on assessing forest structure using various laser scanning platforms. We give suggestions on how to minimise occlusion in various scanning scenarios and highlight exciting research opportunities that arise when explicitly considering occlusion for assessing forest structure.

2. Defining occlusion: what is happening to laser pulses?

Laser scanning data of forests are typically obtained from ground-based, stationary (multi-station) TLS or mobile laser scanning (MLS) acquisitions or from aerial platforms, such as drones or air-planes (ULS, airborne laser scanning (ALS)). The different view-points and sensor characteristics can have various consequences and magnitudes regarding occlusion (see Section 3). Occlusion occurs when objects that could be detected by a laser beam are missed because the beam is blocked by intervening objects. This results in gaps within the point cloud, which are not truly empty but rather artifacts of the scanning process. Figure 1 schematically illustrates the interaction between laser pulses of a TLS acquisition and the causes for the different types of occlusion. Three fundamental types of occlusion can be distinguished based on their causes: absolute, geometric, and sub-footprint occlusion (Figure 1).

Absolute occlusion occurs when a laser pulse is entirely blocked or absorbed, making it impossible to overcome using any scanner technology or acquisition protocol. For example, neither the interiors of tree trunks can be captured by laser scanning, nor underwater objects if the pulses were absorbed. These prevent exploration of underwater objects with standard infrared LiDAR systems.

Geometric occlusion occurs when objects are between the laser scanner and the target volume, but the occluding effect could be overcome if the target were observed from another viewing direction. This type of occlusion is largely determined by the structural arrangement of the vegetation. An

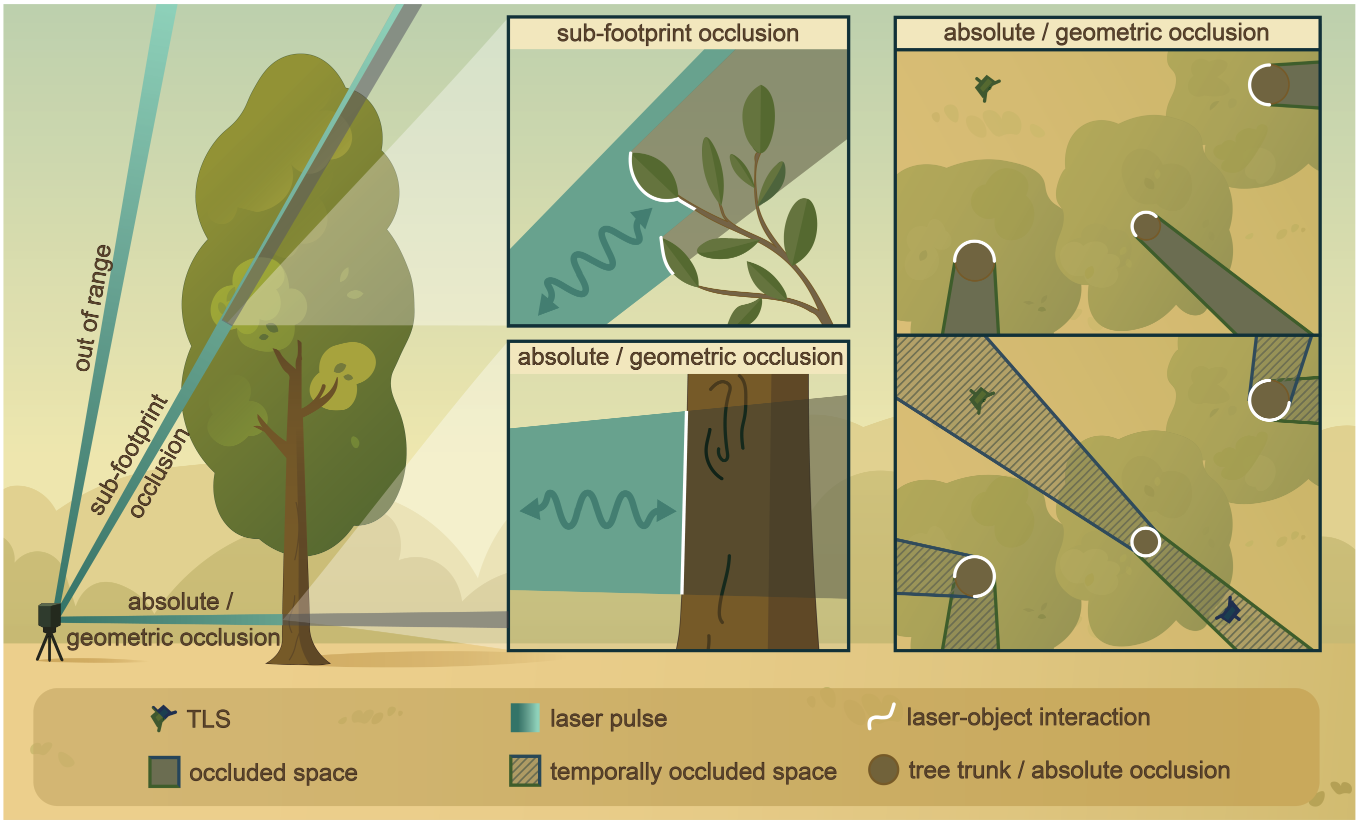

Figure 1: Definition of different occlusion types. Left part of the figure shows the three different occlusion types from a laser beam perspective. Note that the laser beam dimensions are exagerated for visualization purposes. The right side of the figure shows the difference between absolute and geometric occlusion from a single and multi-station TLS acquisition as shown from a top view perspective. Geometric occlusion found in the single station setup (top-right box) can be overcome by an additional scan station, hence these areas were only temporally occluded. The outline of the occluded area is coloured based on the colour of the TLS that cannot observe this area.

example would be the volume behind a trunk when observed from only one side with e.g. TLS. With an additional scan position, this volume could be observed, as shown on the right side of Figure 1.

Sub-footprint occlusion involves beams that are not completely blocked but are partially absorbed or scattered (see top inset on the left side of Figure 1), causing their returned energy to fall below the LiDAR's detection

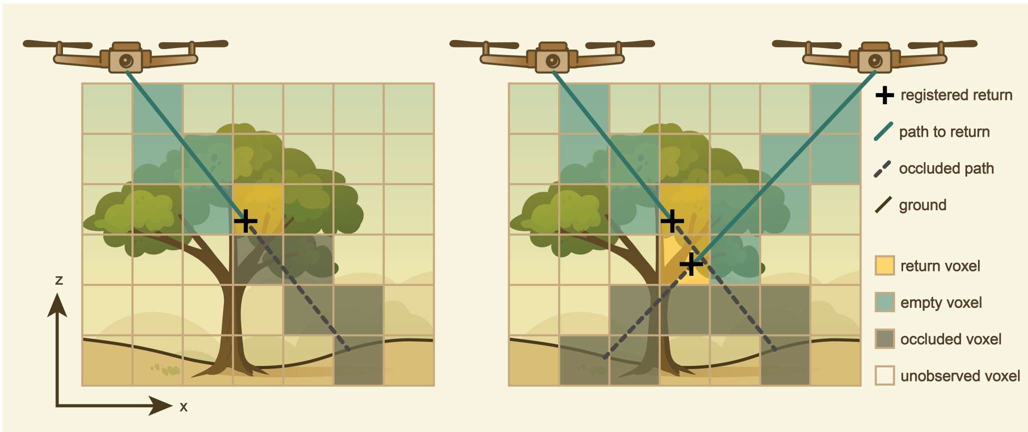

Figure 2: Schematic figure for a voxel traversal algorithm to map occlusion, indicating empty, return, occluded, and unobserved voxels. Left figure shows the voxel traversal and classification of a single pulse emitted from a single location. The right figure shows the same situation with two emitted pulses from two positions. By adding multiple pulses, voxels that have been occluded can be re-classified as observed.

threshold. This occurs when laser pulses strike the edges of objects, which is particularly significant in forests where leaves present a fragmented set of surfaces. The extent of partial occlusion depends on the characteristics of both the laser scanner (e.g. laser pulse power, beam divergence, detector sensitivity) and the material through which pulses are passing (e.g. reflectivity, degree of fragmentation). There is also the case when objects are out of range for the scanner. Here, similarly to partial occlusion, insufficient energy is returned to the detector. Since no objects are in between the potential target and the scanner, this scenario is not considered as occlusion.

Currently, occluded forest volumes are not captured in standard point cloud formats such as LAS or PLY data. A relatively simple way to evaluate the scanned 3D space in respect to occlusion is to discretize the forest volume in a so-called voxel grid. A voxel is basically a 3D representation of a pixel with a pre-defined dimension. By applying a simple voxel traversal algorithm as e.g. introduced by Amanatides and Woo (1987), each laser pulse can be traced through the voxel grid and each voxel can be classified into occluded (hidden), empty (open) and unobserved space by following a classification scheme introduced by Bienert et al. (2010). This concept is illustrated in Figure 2, where the voxel traversal and classification approach is schematically visualized for two laser pulses emitted from an ULS drone from two different viewpoints. Note that, in contrast to empty space, unobserved space cannot be explored because no laser pulses are emitted in this direction. Such volumes should be mitigated by a well-designed scan design and ideally account for a negligible volume fraction.

3. Causes of occlusion and strategies for mitigation

Occlusion in forest environments can never be entirely avoided, and a fully representative 3D reconstruction of a scene is likely unachievable. The magnitude and spatial occurrence of occlusion depend on multiple factors: Firstly, the vegetation structure (i.e., the structural complexity, the density and the spatial arrangement) defines the setting for laser scanning. Secondly, the data acquisition strategies influence the actual resulting occlusion. Thirdly, the technical properties of the laser scanning system (i.e., beam divergence and supported pulse rates) determine the theoretical capabilities of sampling the 3D space. Some of these factors follow general rules, while others are platform-specific. Additionally, mapping and quantification of occlusion depend on the chosen definitions and methods. While not directly linked to the cause of occlusion, these factors must be considered for its analysis as well. The following subsections provide a brief overview on occlusion causes and mitigation strategies, starting with general considerations on forest structure, followed by data acquisition parameters and strategies, implications of laser beam properties and methodological considerations. Table 1 provides a summary of technical laser scanning properties and their expected effect on occlusion. This section particularly addresses readers with an interest in optimizing field campaigns.

3.1. Forest structure and complexity

The specific forest structure sets the framework in which the effects of laser beam properties (see Section 3.3) and data acquisition strategies (see Section 3.2) need to be elucidated. The density and structural complexity of vegetation largely determine the degree of occlusion in relation to the scanner's position. Small vegetation fragments such as leaves have a higher chance of being missed in sampling or generating of partial beam reflections (sub-footprint occlusion), whereas larger elements such as tree trunks are more likely to cause geometric occlusion. The denser the spatial arrangement of vegetation elements, the higher is the likelihood of beam interception and consequently occlusion. Phenology in deciduous forests causes a high seasonal variability of structural density, whereby laser scans are much more affected by occlusion under "leaf-on" than under "leaf-off" conditions. Among all forest types, the dense structure of evergreen tropical rain forests poses the greatest challenge for scan completeness. In general, prior knowledge on forest structure such as the density and spatial arrangement (e.g., plantation forests following a regular grid) is highly beneficial and can be incorporated into data acquisition strategies to reduce occlusion.

3.2. Data acquisition parameters and strategies

Sampling density describes the number of laser beams used to sample a given volume. It is influenced by sensor properties and data acquisition strategies (see Table 1). An increased sampling density achieves a higher spatial resolution and exploitation of small gaps in the forest structure. This results in a more comprehensive exploration of space and reduction of occlusion (Gassilloud et al., 2025). The primary feature of laser scanners to affect sampling density is the pulse repetition rate (PRR), which has increased in recent years in commercial systems. While for many systems the PRR is fixed, for some it can be varied by the user (usually forming a trade-off with the pulse energy and thus the maximum measurement range). Nevertheless, the blocking of beams through an object cannot be overcome by a higher sampling density from the same viewpoint. Instead it may lead to redundant sampling of known space with limited benefits on occlusion reduction. Therefore the main acquisition strategy to increase sampling density typically incorporates scanning from new viewpoints.

Viewpoints are the positions from which a sensor can sample space with its respective field of view (FOV). An increased number and optimized spatial arrangement of viewpoints is the fundamental approach to reducing geometric occlusion in any LiDAR scan (Brede et al., 2022; Gassilloud et al., 2025). Ideally new viewpoints can observe areas that were occluded from previous viewpoints.

For **above-canopy** flying ALS and ULS, the primary challenge is to overcome the blocking effect of the canopy. Figure 3 shows an example of point clouds and occlusion patterns for ULS surveys under both leaf-off and leaf-on conditions. While the system is able to penetrate relatively well into the canopy under leaf-off conditions, it encounters more occlusion in the lower part of the canopy caused by the dense foliage in leaf-on conditions. The coniferous trees which dominate on the left side of the depicted transect clearly show a high amount of occlusion for both acquisitions, whereas the deciduous trees dominating the right side of the transect show an increased amount of occlusion under leaf-on conditions. This indicates the phenological and forest type dependent variations in occlusion patterns (Section 3.1).

The most effective strategy to reduce occlusion is to increase the number of new viewpoints by adding additional flight lines. If there are no preferences on domain-specific sampling, configurations are typically chosen to achieve uniform sampling and viewpoint distribution over the area of interest. This is usually realized by a regularly arranged grid of flight lines, i.e., regularly spaced parallel flight lines, crossed by a 90° rotated second set of lines, which can be complemented by a second double grid rotated by 45° (Brede et al. 2022; Gassilloud et al. 2025). If the sensor's FOV can be adapted, it is recommended to utilize the maximum possible scan angles (Gassilloud et al., 2025), while ensuring that scanner range limits are not exceeded at flight line edges.

Flights conducted at high altitudes deal with several factors that tend to increase occlusion. With increasing beam travel distance, inherent beam divergence reduces the pulse power per unit area, while the greater spacing between consecutive pulses lowers the sampling density. Lower flight altitudes decrease the sensor's FOV overlap if no additional flight lines are added. Kükenbrink et al. (2017) recommended a lateral flight strip overlap of at least 50% for ALS campaigns in order to guarantee that every point in space is at least observed from two different viewing directions. For ULS campaigns, much higher FOV overlaps are usually recommended and possible (e.g. Brede et al., 2022; Gassilloud et al., 2025).

For **ground-based laser scanning** acquisitions, occlusion is typically found towards the top of canopy, within dense tree crowns and in dense understory vegetation. Figure 4 shows an example of point clouds and occlusion patterns resulting from ground-based laser scanning under leaf-off and leaf-on conditions for the same transect as also shown in Figure 3. The leaf-off TLS acquisition exhibits only minimal occlusion within tree trunks and towards the top of the crowns of coniferous trees, thanks to optimal sensor specifications (multi-return, narrow beam-divergence) and dense scanner placement

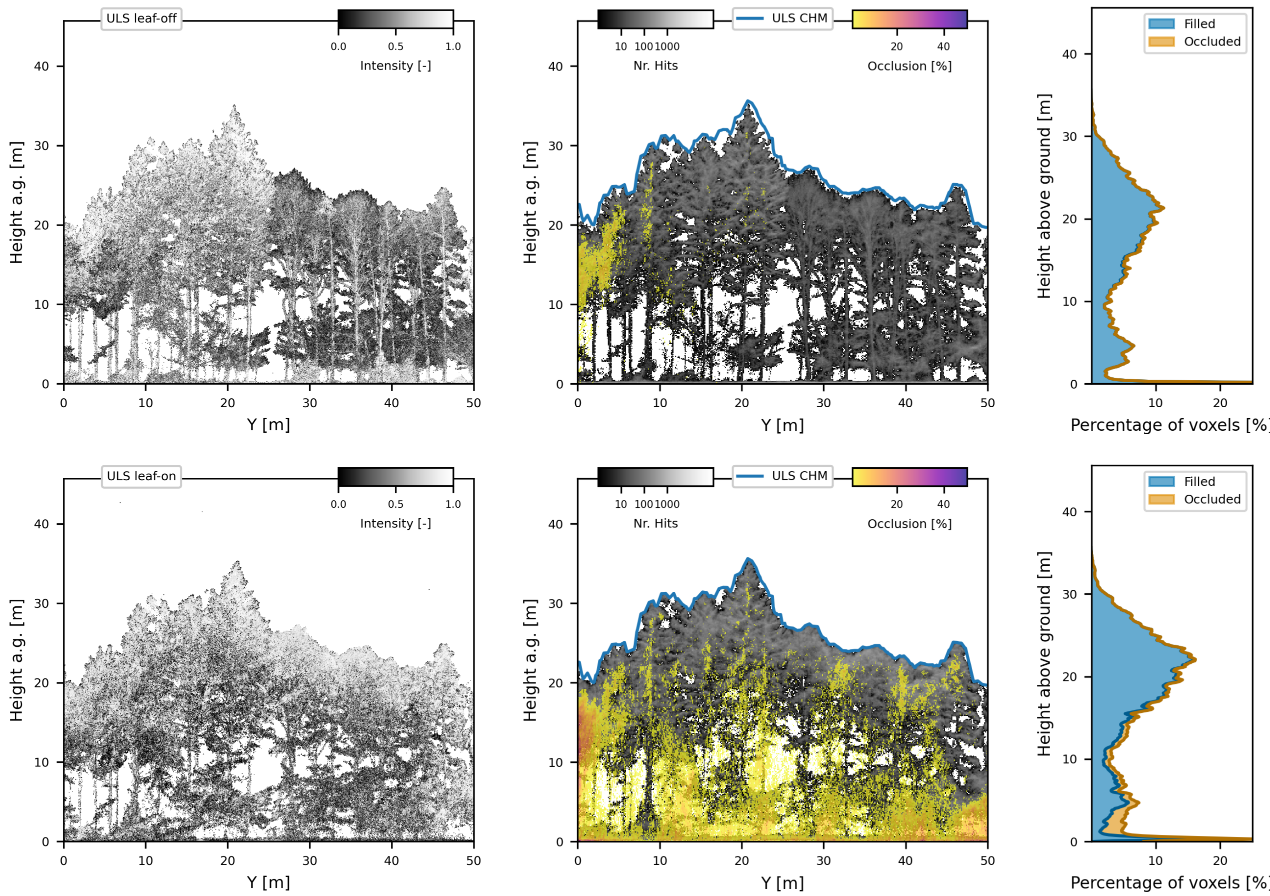

Figure 3: ULS point cloud (left, points coloured based on normalise laser return intensity) and occlusion example for leaf-off (top-row) and leaf-on (bottom) for a 10 m deep transect acquired using a RIEGL miniVUX-3 scanner. The middle column shows the percentage of occluded voxels in relation to the transect depth. Right column shows the cumulative profiles for occluded and filled voxels. White space denotes empty voxels, adding up to 100% of the canopy volume.

(10 m maximum distance between scanner positions). The handheld MLS acquisitions suffer more from occlusion towards the canopy top, also for deciduous trees (right side of the transect), as the single-return system with a larger beam footprint, compared to the TLS system, struggles to penetrate through the denser part of the upper canopy.

For multi-station TLS surveys, occlusion is primarily controlled by the instrument positioning and by sensor settings. Viewpoints are limited to the combination of single scan positions, and their spatial density and strategic placement are the key elements for reducing occlusion. However, station setup and potential target placement to aid scan-station registration are time intensive. Therefore, researchers aim to optimize sensor positioning to either retrieve the best possible result with a given number of scans (Abegg et al., 2017; Wilkes et al., 2017) or to increase the number of scan positions just to the amount where the desired result can be obtained (Li et al., 2020). Often, a regular grid for sensor placements is chosen (Wilkes et al., 2017), due to a lack of prior knowledge on forest structure and better target visibility for co-registration. This strategy is supported by observational evidence (Wilkes et al., 2017) as well as simulations (Abegg et al., 2017). When the forest structure is known in advance, scan positions can be iteratively determined and optimized to efficiently cover occluded areas (Li et al., 2020).

Ground-based MLS surveys share similarities to multi-station TLS surveys in terms of point and occlusion distribution within the canopy. However, compared to TLS acquisition, due to its mobile acquisition strategy of MLS, it is easier to add further viewpoints by moving around the acquisition area. Various acquisition patterns have been reported in previous studies. Their selection is often strongly defined by the shape of the evaluated plot, resulting in a circular acquisition pattern for circular plots, whereas a grid-like pattern is typically employed for rectangular plots. Various variations of these two main approaches were reported by adding petal-like patterns to the acquisition (e.g. Gollob et al., 2020) or through the addition of more parallel lines and directions to the grid patterns (e.g. Mokroš et al., 2021). Sofia et al. (2024) reported that a star-shaped acquisition showed better performance for the estimation of canopy height compared to grid-shaped acquisitions due to the higher number of viewing angles.

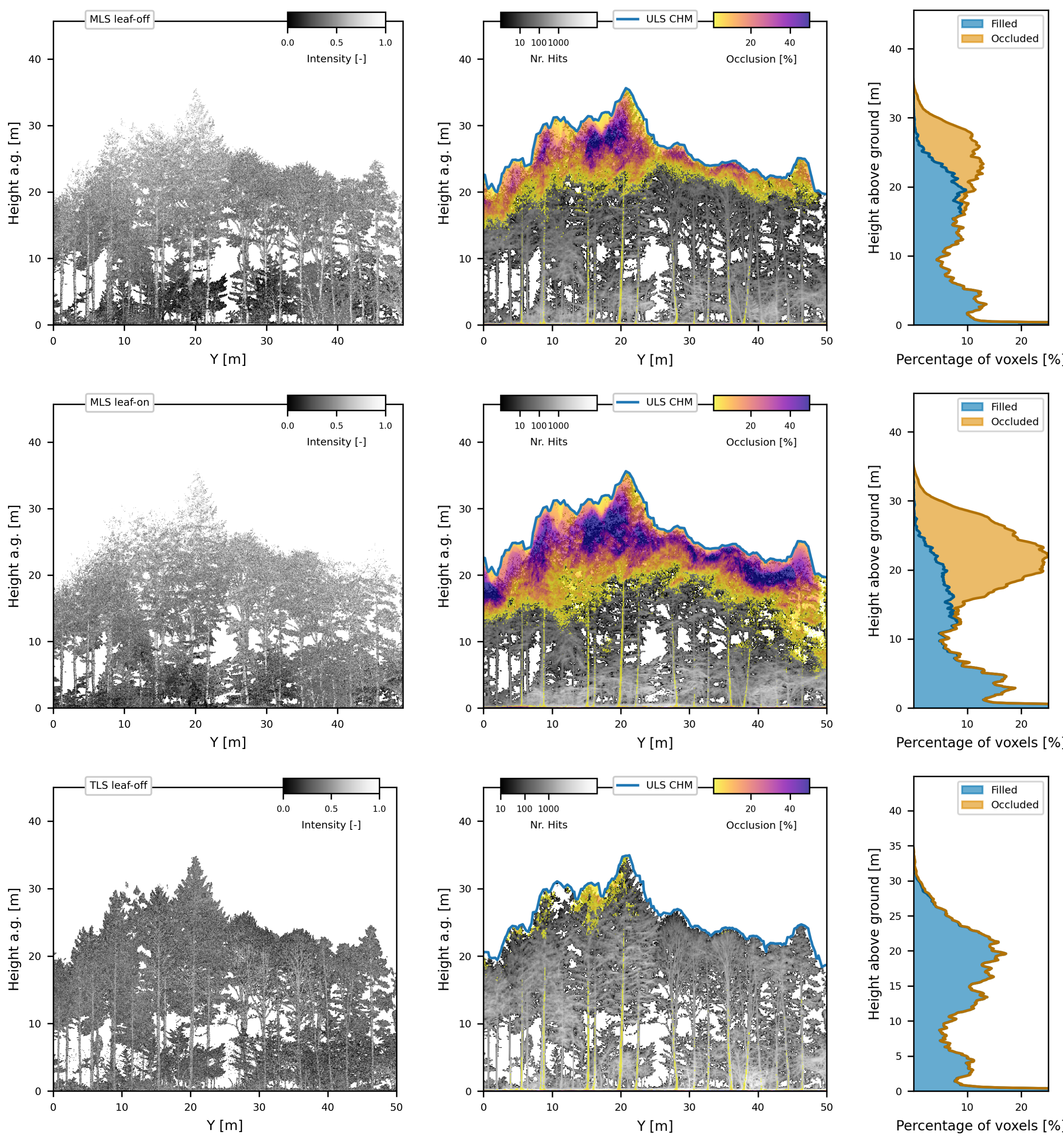

Figure 4: Ground based laser scanning point cloud (left, points coloured based on normalised laser return intensity) and occlusion example for MLS leaf-off (top-row), MLS leaf-on (middle), both acquired using a GeoSLAM ZebHorizon handheld scanner, and TLS (bottom - RIEGL VZ400i) for a 10 m deep transect. The middle column shows the percentage of occluded voxels in relation to the transect depth. Right column shows the cumulative profiles for occluded and filled voxels. White space denotes empty voxels, adding up to 100% of the canopy volume.

The best way to reduce geometrically occluded areas is the **combination of multiple perspectives** from above and below canopy, as they complement each other. Schneider et al. (2019) demonstrated that occlusion could be reduced to <2% with a combination of ground and above canopy laser scans in tropical and temperate forests. This is also shown in Figure 5 where the leaf-on MLS and ULS acquisitions shown in Figures 3 and 4 were combined in order to reduce the areas of occlusion of the respective acquisitions. Therefore, also fusion of TLS and ULS has been proposed in recent studies(Terryn et al., 2022; Yrttimaa et al., 2020). Another approach is scanning at different heights (e.g. via poles, scaffolds or canopy cranes) which can enhance penetration especially in the crown area (D'hont et al., 2025; Schneider et al., 2019; Yun et al., 2019). However, these combination and fusion methods come with the challenge and errors of co-registering the scans from different viewpoints and potentially different systems.

These general strategies for mitigating geometric occlusion come with limitations, as some parameters form complex inter-relationships and have a direct impact on others. Furthermore, logistics and budget typically constrain the acquisition time, so that acquisition patterns need to be optimised. For ALS and ULS, acquisition time is limited by flight time restrictions (e.g. battery capacity). For MLS devices which are reliant on simultaneous localization and mapping (SLAM) technology, prolonged and more complex acquisitions could potentially result in issues with misalignments and drifts within the acquired point clouds (Kükenbrink et al., 2025; Mokroš et al.,

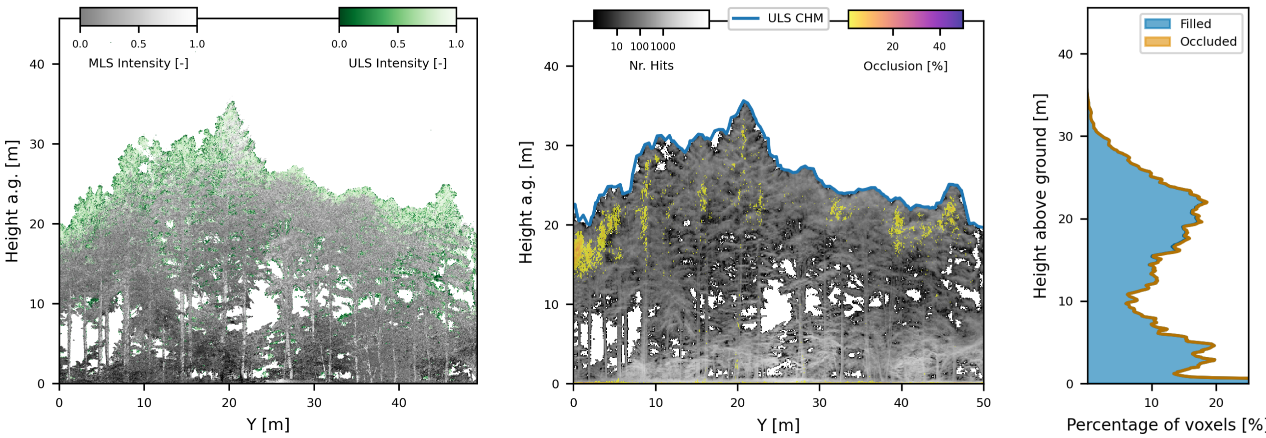

Figure 5: Point cloud and occlusion pattern example for a combination of MLS (GeoSLAM ZebHorizon) and ULS (RIEGL miniVUX-3) acquisitions under leaf-on conditions. The below and above canopy vantage points complement each other to produce a point cloud with minimal occlusion. Individual acquisitions are shown in Figure 3 for ULS acquisition and in Figure 4 for MLS acquisition

2021). Moreover, increased acquisition time for any laser scanning platform may lead to stronger effects from wind-induced vegetation movement, and additional viewpoints result in more frequent co-registration errors.

3.3. Laser beam properties

Laser beam properties are not easily changeable but need to be kept in mind since they impact the processes of beam-canopy interaction including sub-footprint occlusion. For the same forest structure, occlusion patterns will differ depending on the beam properties (Brede et al., 2022). The main scanner parameters to consider are beam divergence (including beam exit diameter), beam energy, pulse duration and the capability to record multiple returns (Table 1).

Abegg et al. (2021) found that for TLS, small objects are less occluded when scanned with smaller beam diameters. Larger beam diameters and hence larger beam footprints often cause multiple objects to be hit by the laser pulse, favouring the identification of the larger objects in the footprint which reflect more energy as well as lowering the spatial accuracy of the generated return (Abegg et al., 2021).

On the other side, at least for multi-return systems, larger beam diameters result in more points per pulse and therefore reduce the geometric occlusion of canopy objects that lie in the line of sight of the emitted beam (Abegg et al., 2021). For such multi-return scenarios, assuming the same footprint size, higher beam energy allows for a higher number of targets, since the cross section of each target decreases with increasing number of targets as the energy is distributed on them (Wagner et al., 2008). Higher beam energy allows detection of more targets by keeping individual returns above the detection threshold, even as the reflected energy of each return weakens with more targets (Wagner et al., 2008). If the energy cross section falls below the threshold of the detector, targets hit by the laser beam cannot generate a return and are therefore occluded.

Finally, the range resolution (shortest separation of objects that can be measured) can result in sensor-specific occlusion of canopy objects. If objects lie within the dead zone from the previous return, they cannot be detected (Wagner et al., 2008). Effects of beam divergence, pulse power, pulse duration and other laser scanning specifications and their interaction are described

Table 1: Laser scanning sensor specifications and their effect on occlusion when increasing the laser scanning specification.

Category	Specification	Definition	Affected properties	Effect on occlusion
Data acquisition parameters	Angular resolution [°][a]	Angular distance between consecutively emitted laser beams	Sampling density	↓
	Pulse repetition frequency [kHz]	Number of pulses sent out per unit of time	Sampling density	↓
	Platform speed [m/s] or [°/sec]	Movement speed of the platform (ALS/ULS/MLS) or rotational speed of the scanner head (TLS)	Sampling density	↑
Laser Beam Properties	Pulse energy [nJ]	Energy of the outgoing pulse	Beam energy distribution, number of returns	↓
	Beam divergence [mrad]	Angular increase in footprint diameter with distance from the aperture	Footprint size, beam energy distribution, multiple returns	↓ ↑
	Pulse duration [ns]	Length of time for a single pulse to be emitted	Minimal detectable distance	↑

[a] For ALS and ULS, the scan line speed [lines/s] is inversely proportional to angular resolution.

in more detail by Morhart et al. (2024), Roussel et al. (2017) and Wagner et al. (2008) based on field experiments, and Abegg et al. (2021), Disney et al. (2010) and Hancock et al. (2015) based on simulation studies.

3.4. Impact of methodology on occlusion mapping and quantification

Mapping occlusion seeks to spatially identify and quantify both explored and unexplored volumes. This is a difficult task, since for an extensive understanding of occluded space, modelling the physical interaction between laser beams and intercepting objects is required. This needs fundamental knowledge on beam properties, such as the energy distribution within a diverging beam, and detailed object characteristics, such as their spatial location, orientation, surface roughness, and optical properties. However, the point cloud is often the only information available, which is insufficient for the accurate reconstruction of laser-object interactions.

Therefore, simplified approaches that trace the trajectory of emitted laser beams through space are commonly used to quantify occlusion. Along the trajectory of a laser pulse, it is necessary to determine whether the beam travelled through empty space, was partially reflected by objects (returns), or reached a point beyond which no or insufficient energy was returned to the sensor (occlusion). The volume, which was traversed by laser beams, can then be mapped according to these respective states. Voxel-based ray tracing algorithms are highly suited for this task, as they allow a very efficient and convenient classification of three-dimensional space and the retrieval of aggregated statistics (see Figure 2 for an illustration of the voxel traversal mechanism).

To map occlusion, emitted laser pulses must first be reconstructed as vectors from their origin to the last return. Thus, knowing the pulse origin, typically given by scan position or trajectory data, is essential for both static and mobile laser scanning systems. If sensor positions are available for mobile acquisitions, the link between laser returns and its respective pulse origin is usually performed through a time flag (i.e. GPS time) available both in the trajectory and the point cloud. By extending the beam vector beyond the last return of the pulse, the occluded part of the laser pulse can be identified. Unfortunately, the provision of sensor positional information is still no standard and can therefore be missing. For this case, or if available vehicle trajectories do not adequately represent sensor position, Gassilloud

Table 2: Voxel classification scheme according to Bienert et al. (2010). Voxels are classified based on the number of hits (i.e. returns) in the voxel, the number of misses (i.e. penetrations that did not generate a return) and occlusions (i.e., rays that could have observed the voxel, but were blocked by other objects closer to the sensor).

	Number of		
	hits (N_{hit})	misses (N_{miss})	occlusions (N_{occ})
Filled	> 0	$\geqslant 0$	$\geqslant 0$
Empty	$= 0$	> 0	$\geqslant 0$
Occluded	$= 0$	$= 0$	> 0
Unobserved	$= 0$	$= 0$	$= 0$

et al. (2025) and Kükenbrink et al. (2017) describe how to reconstruct pulse origin directly from the point cloud. However, these approaches rely on multi-return pulses to reconstruct pulse direction and may introduce uncertainties in estimated sensor positions.

Voxel-based ray tracing algorithms divide space into a 3D grid of voxels. Within each voxel, the number of hits and the traversing occluded and non-occluded beam trajectories are counted. Voxels can be classified according to the user's requirements and definitions. To map completely occluded voxels, a binary classification scheme can be applied, as proposed by Bienert et al. (2010) (Table 2). Other approaches describe voxels with fuzzy membership functions to provide a more comprehensive picture (Béland et al., 2011). Those can be used to identify voxels that are "undersampled" for specific tasks such as leaf area density (LAD)/plant area density (PAD) estimations (see Section 5.3), where a minimum sampling of space is required to retrieve reliable metrics.

Essential for all voxel-based occlusion mapping approaches is the definition of the dimensions of the voxels. The voxel size is a question of scale and has a strong impact on how much of the voxel grid is potentially quantified as occluded (Kükenbrink et al., 2017). With a voxel size too small, many voxels of a grid would potentially not be traversed by laser scanning beams, which subsequently leads to their classification as "unobserved". A voxel size too large hampers the detection of occlusion since larger voxels are more likely to be traversed by beams and therefore be classified as "observed" or "filled". A balanced voxel size enables meaningful analysis and helps identify occluded areas. As a general rule, the voxel size should be considerably larger in linear dimension than the beam width so that they effectively represent the information generated by the scanner. For ALS, a voxel size of 1 m was found to be beneficial (Kükenbrink et al., 2017), while studies investigating high-resolution laser scans with TLS or ULS commonly use a voxel size of 10 cm (e.g. Brede et al., 2022; Kükenbrink et al., 2017; Kükenbrink et al., 2025; Gassilloud et al., 2025; Schneider et al., 2019). The proportion of volume occluded is therefore not only an intrinsic property of the structure and the scanning parameters but also of the subsequent data processing.

Voxel traversal algorithms are straightforward to use but have certain limitations, as they simplify the underlying reality. Due to the inherent beam divergence, LiDAR beams observe larger volumes with increasing distance from the sensor. However, beam trajectories are commonly treated as (infinitesimally small) lines, and the beam divergence is not taken into account. Therefore, the actual explored volume of a LiDAR beam is not captured, and the occurring occlusion is overestimated (Kükenbrink et al., 2017).

Especially for ground-based laser-scanning approaches, empty pulses (i.e. pulses that did not trigger a laser return) can occur, when laser pulses are emitted through canopy gaps into open sky. (This is less of a problem for ULS or ALS acquisitions, as generally every laser pulse will generate at least one return when reaching the ground at the latest.) Not accounting for pulses without returns can result in an overestimation of occlusion and unobserved space. These pulses are absent from point clouds, and often difficult or impossible to extract from raw data of commercial scanners. Moreover, it is generally not possible to distinguish true gaps (where pulses yield no returns) from instances where returns are missing due to instrument-based filtering, where the return signals fall below the scanner's detection threshold. In (Schneider et al., 2019), the extent of overestimation due to not modelling these pulses is investigated in both a temperate and dense tropical forest. They showed that the overestimation is data-dependent, but limited in both forests, and potential bias introduced by misclassification and modelling of near-scanner obstructions as gaps would likely be worse.

This leaves room for improvement and opens up several opportunities for the development of new methods. Future studies might move away from aggregating statistics in a voxel grid and come towards a quantification of "true" observed and occluded volume. This will include the consideration of an (unequal) beam divergence to assess the actual volume explored by the individual laser beams. Further, the energy and its spatial distribution within the laser beam could be taken into account. Assessing the fraction (both energy and footprint) of reflected laser beams as well as the remaining pulse fraction further travelling along the pulse direction has the potential to discretely quantify the occluded 3D space for each laser pulse. By incorporating also full waveform information of laser beams could further aid in the quantification of the "true" occluded space.

4. Occlusion tools

Currently, there are only a few tools available for performing occlusion mapping. Three of these tools were presented at the SilviLaser conference 2023 in London (Brede et al., 2023). The available tools show various stages of implementation, ranging from python (*OccPy* and *CANOPy*) or R (*voxelizeR*) packages up to stand-alone software tools with a fully functional GUI (*AMAPVox*), making it easy for the user to find a suitable tool for their needs. In Table 3 and the following section we present four software tools for occlusion mapping. Other software capable of performing occlusion mapping tasks may exist but have not been tested and evaluated by the authors.

4.1. Occlusion mapping software tools

AMAPVox was initially developed as a stand-alone Java application including a GUI for easy user interaction (Vincent et al., 2017). Since a few years, an R package has been implemented as an interface to the Java based core code. AMAPVox was developed for the estimation of vegetation densities (i.e., PAD/LAD, plant area index (PAI)/leaf area index (LAI)), but its voxel-grid based outputs can be used to create 3D occlusion maps. The tool traces each laser pulse through a pre-defined voxel grid and computes the local transmittance or attenuation for each voxel, from which occlusion information can be retrieved and visualized.

OccPy is a python package where the computationally heavy processing is performed through a C++ implementation of the voxel traversal algorithm introduced by Amanatides and Woo (1987). The interface between the Python and C++ code base is realized through Cython. The tool was initially implemented as Matlab scripts to map occlusion (Kükenbrink et al., 2017) and to estimate vegetation densities from ALS acquisitions (see Table 3 for links to the different tool versions). Later, it was optimized to map occlusion from various platforms and translated into a python package called OccPy.

VoxelizeR is implemented in the R statistical programming language (Brede et al., 2025). It computes the laser's trajectory intersection with the grid lines of the defined voxel grid independent in the three grid dimensions (Brede et al., 2022). It was developed for PAD estimation and occlusion analysis, and interfaces with R's *lidR* and *sf* packages.

CANOPy is a recently published and customizable occlusion mapping tool implemented in Python. It was originally developed for the study in Gassilloud et al. (2025). It is capable of reconstructing sensor position trajectories from point clouds with multiple returns. The module has implemented a box intersection algorithm (Williams et al., 2005) to limit ray tracing to an area of interest and uses the voxel traversal algorithm by Amanatides and Woo (1987).

4.2. On the importance of scan locations and trajectory information for occlusion mapping

As outlined in Section 3.4, for successful occlusion mapping, the trajectory of each laser pulse needs to be reconstructed based on the pulse origin and at least one laser return. Therefore, knowledge about sensor position at all times of the acquisition is essential. We therefore strongly recommend that all users store scanner position or trajectory information (for mobile acquisitions from e.g. ULS, MLS) alongside the acquired point clouds. For selected scenarios, there are approaches available to reconstruct scanner positions if this information is missing or platform movement trajectories do not represent sensor positions well enough (e.g. when the LiDAR sensor is mounted on a moving gimbal with an offset) (e.g. Gassilloud et al., 2025; Kükenbrink et al., 2017). As these reconstruction algorithms rely on multi-return pulses and may introduce uncertainties in sensor position estimates, it is recommended to always store sensor positions, which are often an export option of the processing solutions, alongside the point cloud.

Table 3: Four examples of occlusion mapping software tools with different implementations

Criteria	**AMAPvox**	**OccPy**	**voxelizeR**	**CANOPy**
Height normalisation	Yes	Yes	Yes	Yes
3D plotting outputs	Yes	Yes	No	Yes
Beam size consideration	Yes	No	No	No
Multi-core processing	Yes	Yes (Windows OS)	Yes (Unix-based OS)	Yes
Multiple inputs (point clouds/trajectories)	No	Yes	Yes	Yes
LAD-relevant metrics	Yes	No (occPy) / Yes (in Matlab version)	Yes	No
Graphical user interface	Yes	No	No	No
Manual or vignette	Yes	Yes	Yes	Yes
Test script available	No	Yes	Yes	Yes
Required software	R, AMAPVox	Python, Cython, Conda	R, QGIS	Python, Conda
Ease of installation	Easy	Easy	Easy	Easy
Output file format	`.vox`	`.npy`	`.tif`	`.npy`
Supported OS	Unix, Windows	Unix, Windows	Unix, Windows (no multi-core)	Unix, Windows
Download links	`https://amapvox.org/index.html`	**Python**[a]: `https://github.com/dkueken/OccPy` **Matlab**: `https://www.eufar.net/documents/6028/`	`https://doi.org/10.5281/zenodo.16759585`	`https://github.com/MGEOS/CANOPy`
References	Vincent et al. (2017)	Kükenbrink et al. (2017) Schneider et al. (2019)	Brede et al. (2022)	Gassilloud et al. (2025)

[a] Repository for python version of OccPy is not yet publicly available. It will be published before acceptance of this paper.

5. Research opportunities through occlusion mapping

Rather than solely treating occlusion as a challenge to be overcome, occlusion metrics and mapping can be viewed as an informative feature of acquired point clouds and for assessing vegetation structure. Taking occlusion into account can improve the accuracy of forest metrics, providing a more realistic appraisal of measurements uncertainty, and open up new perspectives on how forest structure can be sampled or studied. In this section, we will discuss various research opportunities highlighting the potential of occlusion mapping for a range of applications.

5.1. Occlusion mapping for smart, autonomous LiDAR data acquisition

During data acquisition, canopy discovery and scan completeness always have to be balanced with scanning time and available personnel, while also avoiding redundancy in collection. Some general guidelines have emerged to achieve this, e.g., regular grid patterns for TLS (Wilkes et al., 2017) and multi-directional grid flight lines for ULS (Brede et al., 2022; Gassilloud et al., 2025). However, while grid patterns appear as intuitively optimal and generally result in a good discovery throughout the area of interest, they do not adapt to spatially variable occlusion. Their implementation is typically time consuming, as the grid size will be chosen conservatively with a focus on the densest forest parts. A few scanning hardware products with live previews already exist, e.g., RIEGL scan map for the VZ-i series (TLS), FARO Stream application for FARO Orbis (MLS), and DJI Pilot application for DJI Zenmuse L2 (ULS). However, they only give an indication of completed areas and preview point cloud density. Point cloud density does not help to indicate the degree of exploration for specific volumes like the crown layer, and empty and occluded spaces cannot be differentiated in point density maps. Here, occlusion mapping could serve as a guidance for efficient data acquisition with completeness in mind. Li et al. (2020) proposed an iterative scanning mode, that optimizes scan positions for maximum volume exploration, aiming at an adaptation to local conditions. Even though this approach only follows a simplified task of detecting trunks at breast height or simplified, circular crown shapes on a horizontal plane while assuming known tree positions, it highlights the future potential with respect to adaptive scan planning.

Recent advances in robotic navigation allow mobile legged robots equipped with LiDAR scanners to perform autonomous forest inventories along human-defined paths. Here, Chirici et al. (2023) showed that the accuracy of tree detection and derived DBH strongly depended on the selected acquisition path. Freißmuth et al. (2024) and Mattamala et al. (2024) presented an online, incremental processing pipeline using a mobile legged robot, allowing for visualisation of forest models during data collection. Such pipelines allow for live decision making and minimisation of occlusion through path modifications by the human operator. Moving one step further, Karjalainen et al. (2025) trialled an autonomous below-canopy flying unoccupied aerial vehicle (UAV). An integration of explicit occlusion mapping into these solutions could improve decision making of the operator, or could further be used for autonomous path planning and adaptation by autonomous platforms to optimize data coverage.

Ideally, a universal optimization approach should target full canopy exploration in order to be agnostic of later analysis objectives, produce results in 3D, and assume no prior knowledge of the forest stand. At the same time, it should take into account requirements for target-less registration between scan positions via point cloud features (e.g., sufficient overlap between individual data takes). Finally, redundant coverage should be minimised. Both registration and occlusion mapping could happen onboard and in real time (Eisoldt et al., 2025). Such an intelligent approach would allow actionable insights and significantly enhance efficiency in both static (i.e., TLS) and mobile laser scanning (i.e., MLS, ULS). Algorithms are becoming available (Section 4) but to be operationally implemented, they must meet high performance standards and demonstrate robustness.

5.2. Quantification of uncertainty with occlusion mapping

Forest structure can be described by a variety of geometrical metrics such as tree height and DBH distribution, layering indices, fractal dimension, quantitative structure models (QSM), gap fraction and density metrics such as plant- or leaf-area densities. All of these metrics can be estimated from point clouds. Therefore, laser scans need to capture the targeted forest structures with sufficient point density and spatial accuracy.

Occlusion can lead to DBH outliers (Heinzel and Huber, 2017; Watt and Donoghue, 2005), a bias in PAD values (Schneider et al., 2019) (see also Section 5.3) and a systematic under-representation of tree height for ground-based systems (Mathes et al., 2023). Currently, point cloud quality and feature representativeness are assessed 1) via sampling density or 2) by comparing point cloud geometries and derived metrics (e.g. DBH, above ground biomass (AGB)) with ground truth data (Dalla Corte et al., 2022; Neuville et al., 2021). Table 4 provides an overview of the severity of occlusion effects on various structural metrics, based on the authors' expert judgment. These are generalizing judgments for very broad categories. Therefore nuances within categories can be expected, mainly due to varying sensor characteristics (see Section 3.3) or data acquisition strategies (see Section 3.2). For example a TLS system capable of producing multiple returns per pulse may suffer less from occlusion for tree height estimation than a TLS system only capable of recording a single return.

While research investigates uncertainty from the perspective of what has been observed, occluded space is often disregarded. Even though the scientific community is aware of uncertainties resulting from occluded space, it is rarely quantified and made use of. Instead, studies tend to accept a certain degree of uncertainty in their data and usually do not recognize the potential of quantifying occluded space to set their work into the context of their laser scanning data.

Actual linkage between quantified occluded space with uncertainties in

Table 4: Expert judgement of the severity of occlusion effects on different structural metrics (low *o*, medium +, high ++) in dependence of the utilized platform.

	Structural metric	Reference	TLS	MLS	ULS/ALS
Tree metrics	**Tree height**	Brede et al. (2017) Davison et al. (2020)	+	+	o
	DBH	Brede et al. (2017) Davison et al. (2020)	o	o	++
	Trunk volume/ stem curve	Prendes et al. (2021)	o	o	++
	Crown projection area	Panagiotidis et al. (2022)	o	o	+
	Crown volume	Panagiotidis et al. (2022)	+	+	+
	QSM	Hartley et al. (2024)	++	++	++
	Leaf area	Frey et al. (2025) Yun et al. (2019)	++	++	++
Plot metrics	**Canopy surface area (DSM)**	Heidrich et al. (2023)	+	+	o
	Canopy cover / gap fraction	Heidrich et al. (2023)	o	o	o
	LAI/PAI	Wang and Fang (2020)	++	++	++
	Occupied/open space	Jung et al. (2013)	+	+	++
	Vertical layering	Knuff et al. (2020)	o	o	+
	Box dimension	Mathes et al. (2023)	++	++	++

estimated forest structural variables has still rarely been performed. The reason is that such a direct relation is often difficult to build. Schneider et al. (2019) linked occluded volume with bias in PAD estimation. However, due to missing reference PAD measurements, a validation of the bias was not possible. We will discuss the specific relation between occlusion and vegetation densities in Section 5.3. Figure 4 also highlights the influence of occlusion towards the typical underestimation of canopy height from below canopy laser scanning acquisitions when compared to ULS derived canopy heights due to the increased occlusion found at the upper canopy layer.

We see quantification of occluded space as a promising tool to identify data gaps, assess uncertainty, and highlight potentially omitted structures. Therefore it has great potential to evaluate point cloud and feature representativeness and link missing information to possible errors of derived metrics. Future studies should further invest in the evaluation of how occluded space affects estimated forest structural variables and their uncertainties.

5.3. Vegetation density metrics

Estimating vegetation densities is crucial for understanding vegetation structure and function in ecological studies. The 3D distribution of vegetation can be described by LAD or - in case leaf and wood material cannot be discriminated - PAD. These parameters have been estimated through various methods based on a similar theoretical background which describes the exponential attenuation of transmittance in a uniform medium along the path of a laser beam, also known as Beer's law (Béland et al., 2011; Pimont et al., 2018; Soma et al., 2021). Most models aiming to estimate 3D LAD or PAD are following a voxel based approach (e.g. Vincent et al., 2017). However, also in this context, a critical challenge is the issue of occlusion. Several studies reported a significant underestimation of LAD or PAD in the upper part of the canopy for ground-based systems or in the lower part of the canopy for above canopy systems (Béland et al., 2014; Schneider et al., 2019; Soma et al., 2020, 2021). The increased underestimation is attributed to insufficient sampling of individual voxels, as pulses are often occluded earlier along their optical path (Béland et al., 2014; Soma et al., 2018, 2021).

A straightforward approach to address this issue would be to increase the voxel size, thereby raising the likelihood that pulses traverse affected voxels. However, Soma et al. (2021) analytically demonstrated through simulations that using larger voxels, while increasing sampling rates, can actually lead to even greater underestimation due to the more heterogeneous distribution of vegetation within each voxel. The authors therefore suggested a voxel size of close to 0.5 m (at least for TLS based LAD and PAD estimations) as a good compromise between increasing sampling density and accounting for heterogeneous distribution of vegetation material within the voxel. A further strategy to increase sampling density and therefore mitigate biases in LAD or PAD estimations is to increase sampling density through a denser scanning pattern (i.e. generating more viewing directions) (Wilkes et al., 2017; Schneider et al., 2019). Also, various approaches have been introduced to compensate biases due to insufficient sampling, ranging from a simple filling of occluded voxels with an average LAD or PAD of explored voxels at a given height (Béland et al., 2014; Schneider et al., 2019), through more sophisticated kriging interpolation approaches (Soma et al., 2020) up to employing light transmission (Béland et al., 2011) or architectural (Côté et al., 2011) models. Yet, all these compensation approaches rely on the knowledge of the spatial distribution of occluded voxels, therefore highlighting the importance of occlusion mapping approaches to gain insights on sampling and occlusion patterns.

5.4. Time series analysis

In recent decades, most forest research involving laser scanning has focused on processing point cloud data and deriving forest and tree structural metrics from one time step. However, as multi-temporal laser scanning datasets become increasingly available, research is gradually shifting towards analyzing changes in these structural metrics over time (e.g. forest and tree structural dynamics). Despite increasing availability, quantifying forest dynamics and structural change from such data remains a complex and unresolved challenge. One of the key obstacles lies in the issue of data interoperability (Bartholomeus et al., 2022). Over the years, a wide range of laser scanning sensors has been developed for various platforms, each with its own specifications and characteristics. As a result, data collected at different time points may have been acquired using different scanners (Huertas et al., 2022; Loh et al., 2022; Yin et al., 2024; Qi et al., 2023). Additionally, due to time constraints or optimized field protocols, data may have been gathered using coarser scanning grids or alternative settings (e.g., faster scanning speeds). Beyond these technical factors, the forest structure itself evolves over time due to seasonal variation (Figure 6), tree growth, and mortality, all of which can significantly affect point cloud quality in terms of a complete representation of the forest canopy. Point cloud quality in multi-temporal datasets can differ substantially, often due to a combination of technical factors and structural forest changes. As a result, point cloud completeness and occlusion can vary substantially between acquisitions of the same site over

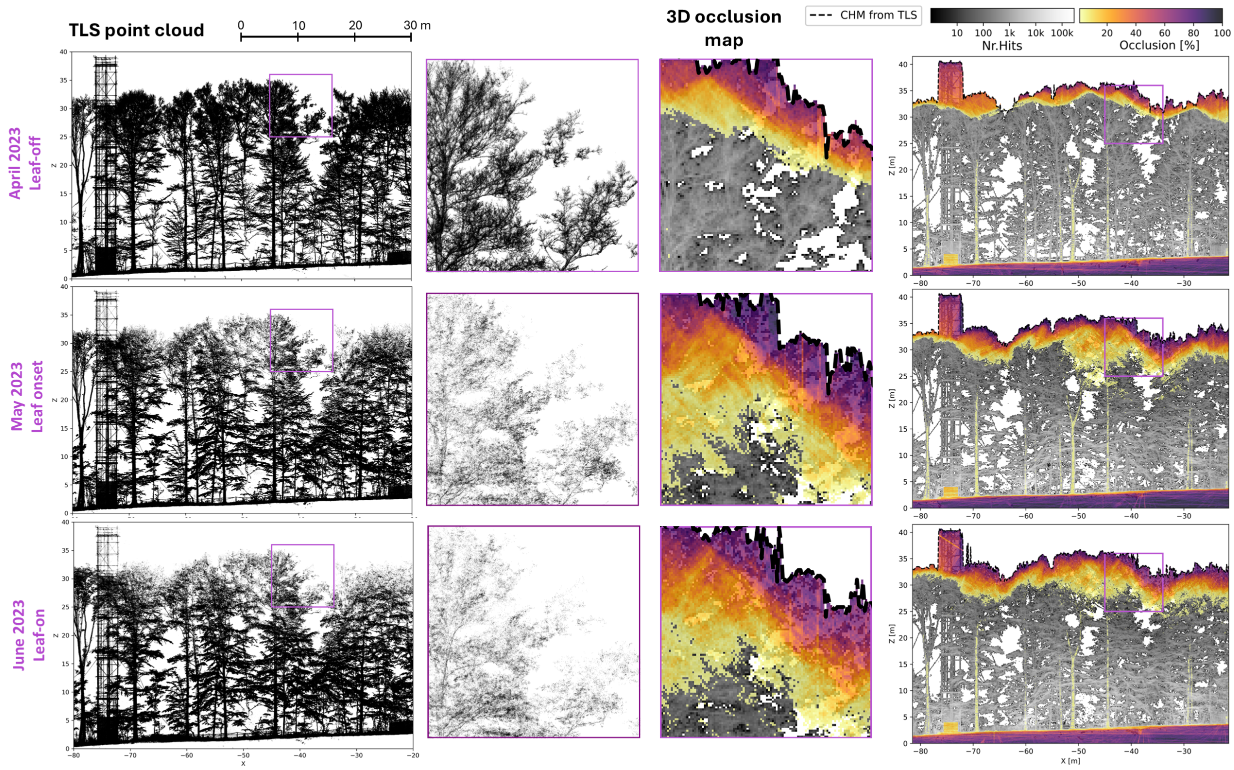

Figure 6: Illustration of the impact of leaves and forest structure on occlusion patterns using a multi-temporal terrestrial laser scanning (TLS) dataset from a temperate deciduous forest in Belgium, showing data from April (leaf-off), May (leaf onset) and June (leaf-on) on the top, middle and bottom, respectively. TLS point cloud data with zoom-in on an area in the top of the canopy (left) and their respective occlusion maps (right) show increased occlusion with leaf onset. Notably, occlusion can also be affected by the angles of the leaves and branches which change when more leaves appear and might reduce or increase occlusion in certain spots.

time, which can, in turn, affect the accuracy of detected changes.

Differences in errors associated with structural measurements from point clouds at different time steps are particularly critical when direct measurements are used (Loh et al., 2022; McRoberts et al., 2015). For example, if tree height is underestimated more in the first time step than in the second, the calculated change in tree height may be significantly overestimated.

Therefore, differing occlusion characteristics pose a major challenge for this approach unless the effects of occlusion are properly detected, quantified, and incorporated into the analysis. In other words, the central challenge in time series analysis is to minimize the uncertainties involved in distinguishing true changes from acquisition-related artefacts as effectively as possible. Quantifying occlusion provides critical insights into the representativeness of the point cloud and specific parts of it, enabling the rejection of apparent changes that arise from differing patterns of occluded space. This perspective becomes especially important when scanning conditions within the time series vary greatly, for example, when combining data from both leaf-on and leaf-off periods (Figure 6) or when incorporating datasets from different sensor types with their associated technical differences.

Occlusion mapping of multi-temporal laser scanning data can provide valuable insights into the differences in measurement uncertainty across time steps, which ideally should be incorporated into an overall uncertainty metric when quantifying change. This approach helps define the minimal amount of change or time difference required for changes to be reliably detected. Additionally, occlusion mapping can assist in determining the area of interest for analysis. For example, by mapping occlusion from leaf-off scans, we can identify the parts of the landscape that are theoretically scanable — that is, the full area the laser can reach without leaf interference. When analyzing summer scans of the same area, the analysis can then be restricted to these parts or adjusted to account for the occluded regions. Furthermore, differences in occlusion across multi-temporal datasets can also be used to explore the type of occlusion (geometric vs. full), since vegetation movement throughout the day can alter occlusion patterns.

5.5. Data prediction and point cloud completion

Various strategies have been developed not only to handle uncertainties in point cloud data but also to interpolate or reconstruct missing information arising from unobserved space during post-processing. Many of these approaches could benefit substantially from an explicit quantification of occlusion and unobserved space. Besides the previously mentioned approaches to compensate biases in vegetation density metrics, in the context of single tree reconstruction various methods have been proposed to infer structural information from incomplete point clouds. These approaches attempt to compensate for data gaps caused by occlusion, often by relying on morphological knowledge and growth patterns of trees. Approaches include algorithms that aim to reconstruct tubular shapes from noisy and occluded point clouds (Ravaglia et al., 2017) or cover the occluded regions of tree stems with an a priori model (Morel et al., 2018). Algorithms grounded in the topology of tree skeletons are also often employed to bridge gaps in the tree structure (Cao et al., 2022; Wang et al., 2023).

In general, 3D reconstruction algorithms aimed at approximating the surface or tree volume represented by the point cloud may benefit from distinguishing gaps caused by open space and gaps caused by occlusion, where assumptions about tree architecture must be made. The same goes for graph-based instance segmentation methods, where data gaps pose a major problem for segmenting individual trees from the forest. How these gaps are handled is data-dependent and often controlled by some user-set parameter, where a balance must be struck between low values leading to oversegmentation and high values leading to undersegmentation, e.g. merging of smaller trees into one instance. Occlusion mapping may be useful in this application by providing a clear distinction between open space gaps, and gaps caused by occlusion.

Recent advances in deep learning have led to the development of point cloud completion networks that aim to reconstruct the full geometry of individual trees from partial observations (Xu et al., 2025; Zhang et al., 2025). These models are trained on large datasets of complete and partial tree point clouds (derived from real or simulated data) to learn structural priors and generate missing points. The completed point clouds can subsequently serve as input for a wide range of downstream analyses. For instance, Bornand et al. (2024) applied a deep learning-based point cloud completion approach to mitigate small scale gaps in dense point clouds of broadleaf trees. Partial and complete point clouds were derived from synthetic tree generation and laser scanning simulation and used to train the transformer-based PoinTr model. Results show the potential of deep learning for completion of partial point clouds. Integration of occlusion mapping results may further improve these models, by explicitly identifying the spatial regions requiring completion. This strategy is particularly useful when applied at the forest plot or stand level, where individual tree segmentation was not performed in advance. In such cases, occlusion mapping can be used to identify sparse regions of the point cloud, allowing the model to target only those areas and thereby avoiding the computational burden and potential noise of processing the entire scene. A more advanced approach could even involve directly integrating occlusion mapping information into the model architecture itself.

Moreover, it remains an open question whether point cloud completion as a preprocessing step could potentially improve the performance of graph-based instance segmentation methods. Future research should investigate whether filling occluded regions leads to better-defined individual tree instances and more accurate segmentation results. An alternative to reconstructing complete point clouds would be to use state-of-the-art deep learning models to directly estimate target variables (such as above-ground biomass or vegetation density) from incomplete data. For such applications, it is essential to develop models that can tolerate missing information and incorporate occlusion bias. In this context, occlusion mapping would again serve as a critical component, providing models with a quantifiable measure of data incompleteness.

However, the success of any data-driven approach fundamentally depends on the availability of large quantities of complete, representative training data. Assessing the completeness and quality of such data remains a major challenge. Currently, visual inspection is the most common method, but systematic occlusion mapping could provide a more robust and objective measure of training data quality in the future. Another promising avenue for generating suitable training and validation datasets is the use of virtual laser scanning, which is discussed in the following subsection.

5.6. Virtual laser scanning to advance the study of occlusion

An inherent problem in occlusion mapping, and thereby also the development of evaluation tools and methods for compensation, is the lack of reference data on what space is occupied by vegetation and what space is empty. While complete coverage is impossible, the best approximation to the required reference data is very dense and high-resolution acquisitions from many viewpoints. Even these still suffer from their own occlusion effects and, since vegetation is not static, come with the challenge of time synchronisation. This makes it difficult to interpret occlusion mapping results in real-world data.

A potential solution to this problem is to simulate laser scanning in virtual vegetation scenes (Figure 7, Winiwarter et al., 2022; Abegg et al., 2023; Wei et al., 2020). We can thereby quantify exactly how much of the vegetation, not just how much of the overall space, is occluded and thus how much relevant information is missing. Virtual laser scanning (VLS) incorporates both necessary metadata for the occlusion mapping tools, such as sensor positions, and full knowledge about the component optical properties. As such, VLS can be used to compare and validate occlusion mapping algorithms and to investigate their sources of error. This includes intermediate technical steps such as assessing the accuracy of the reconstructed rays in the voxel traversal, since the true origins and vectors of each pulse are known.

VLS acts as a virtual playground for designing and evaluating survey strategies and allows systematic and controlled investigation of the different factors influencing occlusion, such as sensor specifications, acquisition settings, and forest structure (Figure 7, Section 3), which are provided as input to the simulations. This enables a better understanding of the magnitude and spatial location of occlusion effects and the effectiveness of approaches to compensation.

In the same way, the effect of occlusion on derived tree and stand-level metrics (see Table 4) can be quantified, since reference data for most of these metrics can be derived directly and automatically from the input VLS scene without error (Winiwarter et al., 2022), and metrics can be compared between VLS scenarios with and without occlusion (Yun et al., 2019). Virtual scenes can be parametrized to replicate real conditions, e.g., tree species, tree height and diameter distributions, and stand densities, which means the effects of occlusion can be investigated for specific forest sites.

All the above analyses require that the simulation, which is always a simplified model of real-world conditions, is sufficiently realistic to effectively reproduce the underlying processes. Thus, while the results need to be confirmed with real experiments, insights from VLS-based sensitivity analyses may allow for informed and cost-effective optimisation of survey plans. While

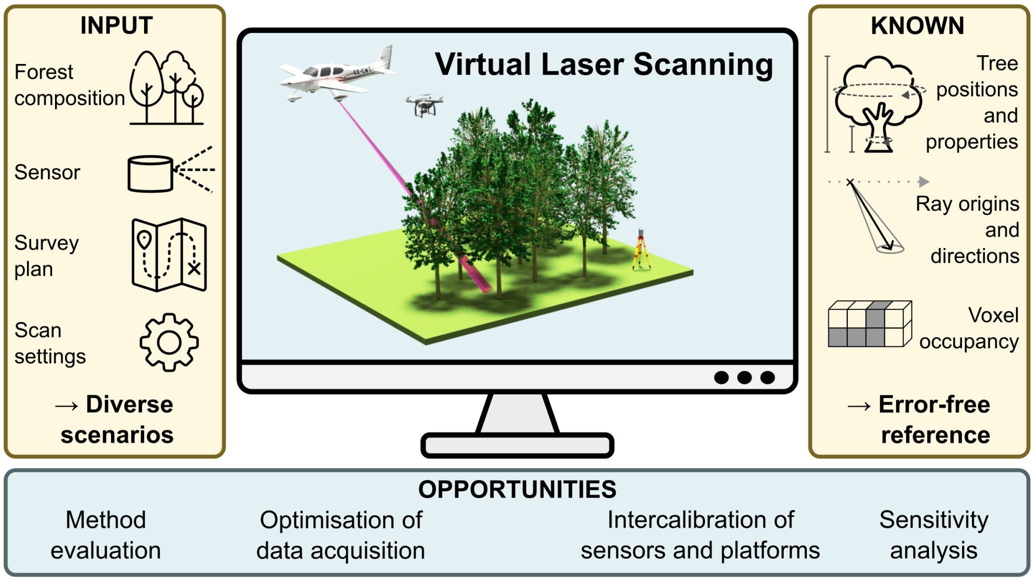

Figure 7: Demonstration of the opportunities from virtual laser scanning (VLS): The operator can vary the composition of the virtual forest, the sensor, the survey plan and the survey settings, enabling diverse and targeted acquisition scenarios (left panel). In the simulated environment, the tree properties, the origins and the directions of the virtual pulses and the occupancy of scene voxels are known and therefore provide error-free reference (right panel). This enables evaluating occlusion quantification methods, conducting sensitivity analyses, and optimising specific data acquisitions.

extremely high-resolution reconstructions of forest scenes from TLS are possible in principle, their creation is highly demanding in terms of field effort and processing time (e.g. Zhu et al., 2023), and the degree of realism required to generate realistic levels of occlusion remains an open question.

6. Conclusion

In this perspective, we have demonstrated that occlusion is a major challenge in forest laser scanning and can heavily affect forest structure analysis and interpretation. By providing a comprehensive review of the concept of occlusion, we set up the theoretical background for a better understanding of its causes, showing the influence of various factors (from forest structure to acquisition strategies, laser instrument properties and interlinked effects). Building upon this, we provided and discussed a range of cross-platform strategies for mitigating occlusion and presented best-practice guidelines for optimized laser scanning acquisitions for forest structure assessment. Our overview of different software tools demonstrated that practical implementations of occlusion mapping are already possible across different programming languages, marking an important step towards greater user accessibility in this field. We further raised awareness that selected metadata information to the point clouds, such as scan position and trajectory information, is essential for occlusion mapping and should therefore be provided and stored alongside the 3D data itself.

Although occlusion is recognized as a major challenge in laser scanning of forests and the retrieval of forest and tree structural parameters, it is rarely explicitly quantified or used as a quality metric of the acquired point clouds. While understanding occlusion and its main drivers is essential for an optimal laser scanning survey, spatial mapping and quantification of occlusion open up a plethora of exciting research opportunities, ranging from point cloud quality assessment, over quantification of uncertainties in point cloud derived forest metrics up to cutting-edge novel research topics on e.g. point cloud completion and virtual laser scanning. We see that through occlusion mapping, new ways to acquire point clouds using adaptive, intelligent acquisition strategies to maximize canopy observation will emerge in the near future, further improving point cloud quality and accuracy of derived forest or tree metrics. We encourage researchers, practitioners, and technology developers to incorporate and advance occlusion-aware approaches, enabling a next generation of forest laser scanning. Given the increasing need to monitor forest structural changes in the face of global change, occlusion mapping may help ensuring robust and reliable extraction of structural information from multi-temporal laser scanning data. These advancements in assessing forest structural dynamics align with the European Union Biodiversity Strategy and the principles of close-to-nature forest management, which emphasize enhancing structural diversity to support forest resilience, long-term productivity, sustainable use, and biodiversity conservation.

CRediT author statement

Daniel Kükenbrink: Conceptualisation, Writing - Original Draft, Writing - Review, Editing, Software, Investigation, Visualization, Supervision & Project administration; **Matthias Gassilloud**: Conceptualisation, Writing - Original Draft, Writing - Review, Editing & Software; **Benjamin Brede**: Conceptualisation, Writing - Original Draft, Writing - Review, Editing, Software & Supervision; **Aline Bornand**: Writing - Review & Editing; **Kim Calders**: Conceptualisation, Writing - Review & Editing; **Wout Cherlet**: Visualization, Writing - Review & Editing; **Markus P Eichhorn**: Writing - Review & Editing; **Julian Frey**: Writing - Review & Editing;

Charis Moana Gretler: Visualization; **Bernhard Höfle**: Conceptualisation, Writing - Review & Editing; **Teja Kattenborn**: Conceptualisation, Writing - Review & Editing; **Lennart Klinger**: Software & Investigation; **Martin Mokroš**: Conceptualisation, Writing - Review & Editing; **Timo P Pitkänen**: Conceptualisation, Writing - Review & Editing; **Ninni Saarinen**: Conceptualisation, Writing - Review & Editing; **Louise Terryn**: Visualization, Writing - Review & Editing; **Hannah Weiser**: Conceptualisation, Visualization, Writing - Review & Editing; **Anna Göritz**: Conceptualisation, Writing - Original Draft, Writing - Review, Editing & Supervision;

Acknowledgements

This article/publication is based upon work from COST Action 3DForEcoTech, CA20118, supported by COST (European Cooperation in Science and Technology). D.K. was supported by the Swiss National Forest Inventory (NFI), a cooperative effort between the Swiss Federal Institute for Forest, Snow and Landscape Research (WSL) and the Swiss Federal Office for the Environment (FOEN). M.G. and A.G. would like to acknowledge funding by the Deutsche Forschungsgemeinschaft (DFG, German Research Foundation) - SFB 1537/1 (CRC ECOSENSE). B.B. acknowledges funding by the European Commission through NextGenCarbon project (grant agreement 101184989). B.H. and H.W. were supported by the Deutsche Forschungsgemeinschaft (DFG, German Research Foundation) in the frame of the projects VirtuaLearn3D (project number: 496418931) and "Fostering a community-driven and sustainable HELIOS++ scientific software" (project number: 528521476). T.K. was supported by the Deutsche Forschungsgemeinschaft (DFG, German Research Foundation) in the frame of the projects LeafH2O (project number: 541018379). N.S. and T.P. were funded by the Research Council of Finland through the UNITE flagship (grant numbers 357906 & 357909). L.T. was funded by Ghent University (Ghent University Bijzonder Onderzoeksfonds Grant No. 01G01923). K.C. and W.C. were funded by the European Union (ERC-2021-STG Grant agreement No. 101039795). Views and opinions expressed are however those of the author(s) only and do not necessarily reflect those of the European Union or the European Research Council Executive Agency. Neither the European Union nor the granting authority can be held responsible for them. Figure 7 shows tree icons made by Freepik, a map icon made by Smashicons, settings icon made by Pixel perfect all available through `www.flaticon.com`. The central 3D scene in Figure 7 is rendered in Blender with an aeroplane model CC-BY Emmanuel Beranger and a drone model by cgtrader.com user `CGaxr`.

Declaration of Generative AI and AI-Assisted Technologies in the Writing Process

During the preparation of this work the author(s) used ChatGPT 4.0/4.1 in order to improve the readability and language. After using this tool/service, the author(s) reviewed and edited the content as needed and take(s) full responsibility for the content of the published article.

References

Abegg, M., Boesch, R., Schaepman, M.E., Morsdorf, F., 2021. Impact of Beam Diameter and Scanning Approach on Point Cloud Quality of Terrestrial Laser Scanning in Forests. IEEE Transactions on Geoscience and Remote Sensing 59, 8153–8167. URL: https://ieeexplore.ieee.org/document/9286414/, doi:10.1109/TGRS.2020.3037763.

Abegg, M., Bösch, R., Kükenbrink, D., Morsdorf, F., 2023. Tree volume estimation with terrestrial laser scanning — testing for bias in a 3d virtual environment. Agricultural and Forest Meteorology 331, 109348. URL: https://www.sciencedirect.com/science/article/pii/S0168192323000424, doi:https://doi.org/10.1016/j.agrformet.2023.109348.

Abegg, M., Kükenbrink, D., Zell, J., Schaepman, M.E., Morsdorf, F., 2017. Terrestrial Laser Scanning for Forest Inventories—Tree Diameter Distribution and Scanner Location Impact on Occlusion. Forests 8, 184. doi:10.3390/f8060184.

Amanatides, J., Woo, A., 1987. A fast voxel traversal algorithm for ray tracing. Proceedings of EUROGRAPHICS 87, 3–10. URL: http://www.cse.yorku.ca/~amana/research/grid.pdf. paper describing the algorithm used for ray tracing!

Barrere, J., Reineking, B., Jaunatre, M., Kunstler, G., 2024. Forest storm resilience depends on the interplay between functional composition and climate—Insights from European-scale simulations. Functional Ecology 38, 500–516. doi:10.1111/1365-2435.14489.

Bartholomeus, H., Calders, K., Whiteside, T., Terryn, L., Krishna Moorthy, S.M., Levick, S.R., Bartolo, R., Verbeeck, H., 2022. Evaluating Data Inter-Operability of Multiple UAV–LiDAR Systems for Measuring the 3D Structure of Savanna Woodland. Remote Sensing 14, 5992. doi:10.3390/rs14235992.

Bienert, A., Queck, R., Schmidt, A., Bernhofer, C., 2010. VOXEL SPACE ANALYSIS OF TERRESTRIAL LASER SCANS IN FORESTS FOR WIND FIELD MODELING. International Archives of Photogrammetry. Remote Sensing and Spatial Information Sciences 38, 92–97.

Bornand, A., Abegg, M., Morsdorf, F., Rehush, N., 2024. Completing 3D point clouds of individual trees using deep learning. Methods in Ecology and Evolution 2024, 1–14. doi:10.1111/2041-210X.14412.

Brede, B., Bartholomeus, H.M., Barbier, N., Pimont, F., Vincent, G., Herold, M., 2022. Peering through the thicket: Effects of UAV LiDAR scanner settings and flight planning on canopy volume discovery. International Journal of Applied Earth Observation and Geoinformation 114, 103056. URL: https://doi.org/10.1016/j.jag.2022.103056, doi:10.1016/j.jag.2022.103056.

Brede, B., Kükenbrink, D., Höfle, B., Kattenborn, T., Klinger, L., Pitkänen, T., Singh, A., Weiser, H., 2023. Occlusion mapping tools for point cloud quality assessment in forest laser scanning, in: SilviLaser 2023, London (UK).

Brede, B., Lau, A., Bartholomeus, H., Kooistra, L., 2017. Comparing RIEGL RiCOPTER UAV LiDAR derived canopy height and DBH with terrestrial LiDAR. Sensors 17, 2371. URL: https://www.mdpi.com/1424-8220/17/10/2371, doi:10.3390/s17102371.

Brede, B., Pimont, F., Vincent, G., Schiedewitz, O., 2025. voxelizer: advanced functionalities for voxelizing lidar point cloud data. URL: https://doi.org/10.5281/zenodo.16759585.

Béland, M., Baldocchi, D.D., Widlowski, J.L., Fournier, R.A., Verstraete, M.M., 2014. On seeing the wood from the leaves and the role of voxel size in determining leaf area distribution of forests with terrestrial LiDAR. Agricultural and Forest Meteorology 184, 82–97. URL: https://linkinghub.elsevier.com/retrieve/pii/S0168192313002608, doi:10.1016/j.agrformet.2013.09.005.

Béland, M., Widlowski, J.L., Fournier, R.A., Côté, J.F., Verstraete, M.M., 2011. Estimating leaf area distribution in savanna trees from terrestrial LiDAR measurements. Agricultural and Forest Meteorology 151, 1252–1266. URL: https://linkinghub.elsevier.com/retrieve/pii/S0168192311001481, doi:10.1016/j.agrformet.2011.05.004.

Calders, K., Adams, J., Armston, J., Bartholomeus, H., Bauwens, S., Bentley, L.P., Chave, J., Danson, F.M., Demol, M., Disney, M., Gaulton, R., Krishna Moorthy, S.M., Levick, S.R., Saarinen, N., Schaaf, C., Stovall, A., Terryn, L., Wilkes, P., Verbeeck, H., 2020. Terrestrial laser scanning in forest ecology: Expanding the horizon. Remote Sensing of Environment 251, 112102. URL: https://linkinghub.elsevier.com/retrieve/pii/S0034425720304752, doi:10.1016/j.rse.2020.112102.

Calders, K., Herold, M., Adams, J., Armston, J., Brede, B., Cherlet, W., Cooper, Z.T., Dayal, K., Frenne, P.D., Levick, S.R., Meir, P., Origo, N., Senf, C., Soenens, L., Terryn, L., Van Den Broeck, W.A., Vastaranta, M., Verbeeck, H., Villard, L., Disney, M., 2025. Realistic virtual forests for understanding forest disturbances and recovery from space. ISPRS Journal of Photogrammetry and Remote Sensing 227, 501–507. doi:10.1016/j.isprsjprs.2025.06.031.

Cao, W., Wu, J., Shi, Y., Chen, D., 2022. Restoration of individual tree missing point cloud based on local features of point cloud. Remote Sensing 14. URL: https://doi.org/10.3390/rs14061346, doi:10.3390/rs14061346. number: 6.

Chirici, G., Giannetti, F., D'Amico, G., Vangi, E., Francini, S., Borghi, C., Corona, P., Travaglini, D., 2023. Robotics in forest inventories: Spot's first steps. Forests 14. URL: https://www.mdpi.com/1999-4907/14/11/2170, doi:10.3390/f14112170.

Côté, J.F., Fournier, R.A., Egli, R., 2011. An architectural model of trees to estimate forest structural attributes using terrestrial LiDAR. Environmental Modelling & Software 26, 761–777. doi:10.1016/j.envsoft.2010.12.008.

Dalla Corte, A.P., de Vasconcellos, B.N., Rex, F.E., Sanquetta, C.R., Mohan, M., Silva, C.A., Klauberg, C., de Almeida, D.R.A., Zambrano, A.M.A., Trautenmüller, J.W., Leite, R.V., do Amaral, C.H., Veras, H.F.P., da Silva Rocha, K., de Moraes, A., Karasinski, M.A., Sanquetta, M.N.I., Broadbent, E.N., 2022. Applying High-Resolution UAV-LiDAR and Quantitative Structure Modelling for Estimating Tree Attributes in a Crop-Livestock-Forest System. Land 11, 507. URL: https://www.mdpi.com/2073-445X/11/4/507, doi:10.3390/land11040507.

Damm, A., Paul-Limoges, E., Kükenbrink, D., Bachofen, C., Morsdorf, F., 2020. Remote sensing of forest gas exchange: Considerations derived from a tomographic perspective. Global Change Biology 26. doi:10.1111/gcb.15007.

Davison, S., Donoghue, D.N., Galiatsatos, N., 2020. The effect of leaf-on and leaf-off forest canopy conditions on LiDAR derived estimations of forest structural diversity. International Journal of Applied Earth Observation and Geoinformation 92, 102160. URL: https://linkinghub.elsevier.com/retrieve/pii/S0303243420300684, doi:10.1016/j.jag.2020.102160.

D'hont, B., Calders, K., Antonelli, A., Berg, T., Cherlet, W., Dayal, K., Fitzpatrick, O.J., Hambrecht, L., Leponce, M., Lucieer, A., Pascal, O., Raumonen, P., Verbeeck, H., 2025. Integrating terrestrial and canopy laser scanning for comprehensive analysis of large old trees: Implications for single tree and biodiversity research. Remote Sensing in Ecology and Conservation n/a. doi:10.1002/rse2.70021.

Disney, M., Kalogirou, V., Lewis, P., Prieto-Blanco, A., Hancock, S., Pfeifer, M., 2010. Simulating the impact of discrete-return lidar system and survey characteristics over young conifer and broadleaf forests. Remote Sensing of Environment 114, 1546–1560. URL: https://linkinghub.elsevier.com/retrieve/pii/S0034425710000684, doi:10.1016/j.rse.2010.02.009.

Ehbrecht, M., Schall, P., Juchheim, J., Ammer, C., Seidel, D., 2026. Effective number of layers: A new measure for quantifying three-dimensional stand structure based on sampling with terrestrial LiDAR. Forest Ecology and Management 380, 212–223. URL: http://linkinghub.elsevier.com/retrieve/pii/S0378112716305102, doi:10.1016/j.foreco.2016.09.003.

Ehbrecht, M., Seidel, D., Annighöfer, P., Kreft, H., Köhler, M., Zemp, D.C., Puettmann, K., Nilus, R., Babweteera, F., Willim, K., Stiers, M., Soto, D., Boehmer, H.J., Fisichelli, N., Burnett, M., Juday, G., Stephens, S.L., Ammer, C., 2021. Global patterns and climatic controls of forest structural complexity. Nature Communications 12, 519. doi:10.1038/s41467-020-20767-z.

Eisoldt, M., Mock, A., Wiemann, T., Porrmann, M., 2025. Efficient global 6d localization in 3d tsdf maps using point-wise and scan-wise reduction methods on embedded gpus. International Journal of Semantic Computing 0, null. URL: https://doi.org/10.1142/S1793351X25410053, doi:10.1142/S1793351X25410053, arXiv:https://doi.org/10.1142/S1793351X25410053.

Freißmuth, L., Mattamala, M., Chebrolu, N., Schaefer, S., Leutenegger, S., Fallon, M., 2024. Online tree reconstruction and forest inventory on a mobile robotic system, in: 2024 IEEE/RSJ International Conference on Intelligent Robots and Systems (IROS), pp. 11765–11772. doi:10.1109/IROS58592.2024.10802455.

Frey, J., Schindler, Z., McClatchy, P., Morhart, C., Larysch, E., Seifert, T., 2025. The 3d reconstruction of wood and leaves from terrestrial laser scanning – a case study on PAR measurements below a solitary malus domestica tree. Silva Fennica 59. URL: https://www.silvafennica.fi/article/24027, doi:10.14214/sf.24027.

Gassilloud, M., Koch, B., Göritz, A., 2025. Occlusion mapping reveals the impact of flight and sensing parameters on vertical forest structure exploration with cost-effective uav based laser scanning. International Journal of Applied Earth Observation and Geoinformation 139, 104493.

Gollob, C., Ritter, T., Nothdurft, A., 2020. Forest inventory with long range and high-speed personal laser scanning (PLS) and simultaneous localization and mapping (SLAM) technology. Remote Sensing 12. doi:10.3390/RS12091509.

Hancock, S., Armston, J., Li, Z., Gaulton, R., Lewis, P., Disney, M., Mark Danson, F., Strahler, A., Schaaf, C., Anderson, K., Gaston, K.J., 2015. Waveform lidar over vegetation: An evaluation of inversion methods for estimating return energy. Remote Sensing of Environment 164, 208–224. URL: https://linkinghub.elsevier.com/retrieve/pii/S003442571500142X, doi:10.1016/j.rse.2015.04.013.

Hartley, R.J.L., Jayathunga, S., Morgenroth, J., Pearse, G.D., 2024. Tree branch characterisation from point clouds: a comprehensive review. Current Forestry Reports 10, 360–385. URL: https://link.springer.com/10.1007/s40725-024-00225-5, doi:10.1007/s40725-024-00225-5.

Heidrich, L., Bae, S., Levick, S., Seibold, S., Weisser, W., Krzystek, P., Magdon, P., Nauss, T., Schall, P., Serebryanyk, A., Wöllauer, S., Ammer, C., Bässler, C., Doerfler, I., Fischer, M., Gossner, M.M., Heurich, M., Hothorn, T., Jung, K., Kreft, H., Schulze, E.D., Simons, N., Thorn, S., Müller, J., 2020. Heterogeneity–diversity relationships differ between and within trophic levels in temperate forests. Nature Ecology & Evolution 4, 1204–1212. URL: https://www.nature.com/articles/s41559-020-1245-z, doi:10.1038/s41559-020-1245-z. bandiera_abtest:

a Cg_type: Nature Research Journals Number: 9 Primary_atype: Research Publisher: Nature Publishing Group Subject_term: Community ecology;Forest ecology;Forestry;Theoretical ecology Subject_term_id: community-ecology;forest-ecology;forestry;theoretical-ecology.

Heidrich, L., Brandl, R., Ammer, C., Bae, S., Bässler, C., Doerfler, I., Fischer, M., Gossner, M.M., Heurich, M., Heibl, C., Jung, K., Krzystek, P., Levick, S., Magdon, P., Schall, P., Schulze, E.D., Seibold, S., Simons, N.K., Thorn, S., Weisser, W.W., Wöllauer, S., Müller, J., 2023. Effects of heterogeneity on the ecological diversity and redundancy of forest fauna. Basic and Applied Ecology 73, 72–79. URL: https://linkinghub.elsevier.com/retrieve/pii/S1439179123000610, doi:10.1016/j.baae.2023.10.005.

Heinzel, J., Huber, M.O., 2017. Tree Stem Diameter Estimation From Volumetric TLS Image Data. Remote Sensing 9, 614. doi:10.3390/rs9060614.

Helbach, J., Frey, J., Messier, C., Mörsdorf, M., Scherer-Lorenzen, M., 2022. Light heterogeneity affects understory plant species richness in temperate forests supporting the heterogeneity–diversity hypothesis. Ecology and Evolution 12, e8534. URL: https://onlinelibrary.wiley.com/doi/abs/10.1002/ece3.8534, doi:10.1002/ece3.8534. _eprint: https://onlinelibrary.wiley.com/doi/pdf/10.1002/ece3.8534.

Huertas, C., Sabatier, D., Derroire, G., Ferry, B., Jackson, T., Pélissier, R., Vincent, G., 2022. Mapping tree mortality rate in a tropical moist forest using multi-temporal lidar. International Journal of Applied Earth Observation and Geoinformation 109, 102780. URL: https://www.sciencedirect.com/science/article/pii/S0303243422001064, doi:https://doi.org/10.1016/j.jag.2022.102780.

Jactel, H., Bauhus, J., Boberg, J., Bonal, D., Castagneyrol, B., Gardiner, B., Gonzalez-Olabarria, J.R., Koricheva, J., Meurisse, N., Brockerhoff, E.G., 2017. Tree Diversity Drives Forest Stand Resistance to Natural Disturbances. Current Forestry Reports 3, 223–243. doi:10.1007/s40725-017-0064-1.

Jung, J., Pekin, B.K., Pijanowski, B.C., 2013. Mapping open space in an old-growth, secondary-growth, and selectively-logged tropical rainforest using discrete return LIDAR. IEEE Journal of Selected Topics in Applied Earth Observations and Remote Sensing 6, 2453–2461. URL: http://ieeexplore.ieee.org/document/6494343/, doi:10.1109/JSTARS.2013.2253306.

Karjalainen, V., Koivumäki, N., Hakala, T., Muhojoki, J., Hyyppä, E., George, A., Suomalainen, J., Honkavaara, E., 2025. Towards autonomous photogrammetric forest inventory using a lightweight under-canopy robotic drone. URL: https://arxiv.org/abs/2501.12073, arXiv:2501.12073.

Kesselring, J., Morsdorf, F., Kükenbrink, D., Gastellu-Etchegorry, J.P., Damm, A., 2024. Diversity of 3D APAR and LAI dynamics in broadleaf and coniferous forests: Implications for the interpretation of remote sensing-based products. Remote Sensing of Environment 306, 114116. doi:10.1016/j.rse.2024.114116.

Knuff, A.K., Staab, M., Frey, J., Dormann, C.F., Asbeck, T., Klein, A.M., 2020. Insect abundance in managed forests benefits from multi-layered vegetation. Basic and Applied Ecology 48, 124–135. URL: http://www.sciencedirect.com/science/article/pii/S143917912030092X, doi:10.1016/j.baae.2020.09.002.

Kükenbrink, D., Marty, M., Rehush, N., Abegg, M., Ginzler, C., 2025. Evaluating the potential of handheld mobile laser scanning for an operational inclusion in a national forest inventory – A Swiss case study. Remote Sensing of Environment 321, 114685. doi:10.1016/j.rse.2025.114685.

Kükenbrink, D., Schneider, F., Leiterer, R., Schaepman, M., Morsdorf, F., 2017. Quantification of hidden canopy volume of airborne laser scanning data using a voxel traversal algorithm. Remote Sensing of Environment 194. doi:10.1016/j.rse.2016.10.023.

Kükenbrink, D., Schneider, F.D., Schmid, B., Gastellu-Etchegorry, J.P., Schaepman, M.E., Morsdorf, F., 2021. Modelling of three-dimensional, diurnal light extinction in two contrasting forests. Agricultural and Forest Meteorology 296, 108230. URL: https://doi.org/10.1016/j.agrformet.2020.108230https://linkinghub.elsevier.com/retrieve/pii/S0168192320303324, doi:10.1016/j.agrformet.2020.108230.

Lefsky, M.A., Cohen, W.B., Parker, G.G., Harding, D.J., 2002. Lidar Remote Sensing for Ecosystem Studies: Lidar, an emerging remote sensing technology that directly measures the three-dimensional distribution of plant canopies, can accurately estimate vegetation structural attributes and should be of particular interest to forest, landscape, and global ecologists. BioScience 52, 19–30. doi:10.1641/0006-3568(2002)052[0019:LRSFES]2.0.CO;2.

Li, L., Mu, X., Soma, M., Wan, P., Qi, J., Hu, R., 2020. An Iterative-Mode Scan Design of Terrestrial Laser Scanning in Forests for Minimizing Occlusion Effects. IEEE Transactions on Geoscience and Remote Sensing 59, 3547–3566. doi:10.1109/TGRS.2020.3018643.

Liang, X., Kukko, A., Balenović, I., Saarinen, N., Junttila, S., Kankare, V., Holopainen, M., Mokroš, M., Surový, P., Kaartinen, H., Jurjević, L., Honkavaara, E., Näsi, R., Liu, J., Hollaus, M., Tian, J., Yu, X., Pan, J., Cai, S., Virtanen, J.P., Wang, Y., Hyyppä, J., 2022. Close-range remote sensing of forests: The state of the art, challenges, and opportunities for systems and data acquisitions. IEEE Geoscience and Remote Sensing Magazine 10, 32–71. doi:10.1109/MGRS.2022.3168135.

Loh, H.Y., James, D., Ioki, K., Wong, W.V.C., Tsuyuki, S., Phua, M.H., 2022. Estimating aboveground biomass changes in a human-modified tropical montane forest of borneo using multi-temporal airborne lidar data. Remote Sensing Applications: Society and Environment 28, 100821. doi:https://doi.org/10.1016/j.rsase.2022.100821.

Mathes, T., Seidel, D., Häberle, K.H., Pretzsch, H., Annighöfer, P., 2023. What Are We Missing? Occlusion in Laser Scanning Point Clouds and Its Impact on the Detection of Single-Tree Morphologies and Stand Structural Variables. Remote Sensing 15, 450. URL: https://www.mdpi.com/2072-4292/15/2/450, doi:10.3390/rs15020450.

Mattamala, M., Chebrolu, N., Casseau, B., Freißmuth, L., Frey, J., Tuna, T., Hutter, M., Fallon, M., 2024. Autonomous forest inventory with legged robots: System design and field deployment. URL: https://arxiv.org/abs/2404.14157, arXiv:2404.14157.

McRoberts, R.E., Næsset, E., Gobakken, T., Bollandsås, O.M., 2015. Indirect and direct estimation of forest biomass change using forest inventory and airborne laser scanning data. Remote Sensing of Environment 164, 36–42. URL: https://www.sciencedirect.com/science/article/pii/S0034425715000772, doi:https://doi.org/10.1016/j.rse.2015.02.018.

Mokroš, M., Mikita, T., Singh, A., Tomaštík, J., Chudá, J., Wezyk, P., Kuželka, K., Surový, P., Klimánek, M., Zieba-Kulawik, K., Bobrowski, R., Liang, X., 2021. Novel low-cost mobile mapping systems for forest inventories as terrestrial laser scanning alternatives. International Journal of Applied Earth Observation and Geoinformation 104, 102512. doi:10.1016/j.jag.2021.102512.

Morel, J., Bac, A., Véga, C., 2018. Surface reconstruction of incomplete datasets: A novel poisson surface approach based on CSRBF. Computers and Graphics (Pergamon) 74, 44–55. doi:10.1016/j.cag.2018.05.004. publisher: Pergamon.

Morhart, C., Schindler, Z., Frey, J., Sheppard, J.P., Calders, K., Disney, M., Morsdorf, F., Raumonen, P., Seifert, T., 2024. Limitations of estimating branch volume from terrestrial laser scanning. European Journal of Forest Research 143, 687–702. doi:10.1007/s10342-023-01651-z.

Morsdorf, F., Kükenbrink, D., Schneider, F.D., Abegg, M., Schaepman, M.E., 2018. Close-range laser scanning in forests: Towards physically based semantics across scales. Interface Focus 8, 20170046. doi:10.1098/rsfs.2017.0046.

Moudrý, V., Cord, A.F., Gábor, L., Laurin, G.V., Barták, V., Gdulová, K., Malavasi, M., Rocchini, D., Stereńczak, K., Prošek, J., Klápště, P., Wild, J., 2023. Vegetation structure derived from airborne laser scanning to assess species distribution and habitat suitability: The way forward. Diversity and Distributions 29, 39–50. doi:10.1111/ddi.13644.

Neuville, R., Bates, J.S., Jonard, F., 2021. Estimating Forest Structure from UAV-Mounted LiDAR Point Cloud Using Machine Learning. Remote Sensing 13, 352. URL: https://www.mdpi.com/2072-4292/13/3/352, doi:10.3390/rs13030352.

Pan, Y., Birdsey, R.A., Phillips, O.L., Jackson, R.B., 2013. The Structure, Distribution, and Biomass of the World's Forests. Annual Review of Ecology, Evolution, and Systematics 44, 593–622. doi:10.1146/annurev-ecolsys-110512-135914.

Panagiotidis, D., Abdollahnejad, A., Slavík, M., 2022. 3d point cloud fusion from UAV and TLS to assess temperate managed forest structures. International Journal of Applied Earth Observation and Geoinformation 112, 102917. URL: https://linkinghub.elsevier.com/retrieve/pii/S1569843222001182, doi:10.1016/j.jag.2022.102917.

Pimont, F., Allard, D., Soma, M., Dupuy, J.L., 2018. Estimators and confidence intervals for plant area density at voxel scale with T-LiDAR. Remote Sensing of Environment 215, 343–370. doi:10.1016/j.rse.2018.06.024.

Pörtner, H.O., Scholes, R.J., Agard, J., Archer, E., Arneth, A., Bai, X., Barnes, D., Burrows, M., Chan, L., Cheung, W.L.W., Diamond, S., Donatti, C., Duarte, C., Eisenhauer, N., Foden, W., Gasalla, M.A., Handa, C., Hickler, T., Hoegh-Guldberg, O., Ichii, K., Jacob, U., Insarov, G., Kiessling, W., Leadley, P., Leemans, R., Levin, L., Lim, M., Maharaj, S., Managi, S., Marquet, P.A., McElwee, P., Midgley, G., Oberdorff, T., Obura, D., Osman Elasha, B., Pandit, R., Pascual, U., Pires, A.P.F., Popp, A., Reyes-García, V., Sankaran, M., Settele, J., Shin, Y.J., Sintayehu, D.W., Smith, P., Steiner, N., Strassburg, B., Sukumar, R., Trisos, C., Val, A.L., Wu, J., Aldrian, E., Parmesan, C., Pichs-Madruga, R., Roberts, D.C., Rogers, A.D., Díaz, S., Fischer, M., Hashimoto, S., Lavorel, S., Wu, N., Ngo, H., 2021. Scientific Outcome of the IPBES-IPCC Co-Sponsored Workshop on Biodiversity and Climate Change. Technical Report. Zenodo. doi:10.5281/ZENODO.4659158.

Prendes, C., Cabo, C., Ordoñez, C., Majada, J., Canga, E., 2021. An algorithm for the automatic parametrization of wood volume equations from terrestrial laser scanning point clouds: application in *Pinus pinaster*. GIScience & Remote Sensing 58, 1130–1150. URL: https://www.tandfonline.com/doi/full/10.1080/15481603.2021.1972712, doi:10.1080/15481603.2021.1972712.

Qi, Z., Li, S., Pang, Y., Du, L., Zhang, H., Li, Z., 2023. Monitoring spatiotemporal variation of individual tree biomass using multitemporal lidar data. Remote Sensing 15. doi:10.3390/rs15194768.

Ravaglia, J., Bac, A., Fournier, R.A., 2017. Extraction of tubular shapes from dense point clouds and application to tree reconstruction from laser scanned data. Computers & Graphics 66, 23–33. doi:10.1016/J.CAG.2017.05.016. publisher: Pergamon.

Roussel, J.R., Caspersen, J., Béland, M., Thomas, S., Achim, A., 2017. Removing bias from LiDAR-based estimates of canopy height: Accounting for the effects of pulse density and footprint size. Remote Sensing of Environment 198, 1–16. URL: https://linkinghub.elsevier.com/retrieve/pii/S0034425717302316, doi:10.1016/j.rse.2017.05.032.

Schneider, F., Kükenbrink, D., Schaepman, M., Schimel, D., Morsdorf, F., 2019. Quantifying 3D structure and occlusion in dense tropical and temperate forests using close-range LiDAR. Agricultural and Forest Meteorology 268. doi:10.1016/j.agrformet.2019.01.033.

Seidel, D., Fleck, S., Leuschner, C., Hammett, T., 2011. Review of ground-based methods to measure the distribution of biomass in forest canopies. Annals of Forest Science 68, 225–244. doi:10.1007/s13595-011-0040-z.

Sofia, S., Giannetti, F., Buscarini, S., Chirici, G., Corezzola, S., Maetzke, F.G., Miozzo, M., Travaglini, D., Veca, D.S.L.M., 2024. Comparing efficiency, timing and costs of different walking paths in HMLS LIDAR survey. Annals of Forest Research 67, 87–107. doi:10.15287/afr.2024.3671.

Soma, M., Pimont, F., Allard, D., Fournier, R., Dupuy, J.L., 2020. Mitigating occlusion effects in Leaf Area Density estimates from Terrestrial LiDAR through a specific kriging method. Remote Sensing of Environment 245, 111836. doi:10.1016/j.rse.2020.111836.

Soma, M., Pimont, F., Dupuy, J.L., 2021. Sensitivity of voxel-based estimations of leaf area density with terrestrial LiDAR to vegetation structure and sampling limitations: A simulation experiment. Remote Sensing of Environment 257, 112354. doi:10.1016/j.rse.2021.112354.

Soma, M., Pimont, F., Durrieu, S., Dupuy, J.L., 2018. Enhanced Measurements of Leaf Area Density with T-LiDAR: Evaluating and Calibrating the Effects of Vegetation Heterogeneity and Scanner Properties. Remote Sensing 10, 1580. doi:10.3390/rs10101580.

Terryn, L., Calders, K., Bartholomeus, H., Bartolo, R.E., Brede, B., D'hont, B., Disney, M., Herold, M., Lau, A., Shenkin, A., Whiteside, T.G., Wilkes, P., Verbeeck, H., 2022. Quantifying tropical forest structure through terrestrial and UAV laser scanning fusion in Australian rainforests. Remote Sensing of Environment 271, 112912. doi:10.1016/j.rse.2022.112912.

Toivonen, J., Kangas, A., Maltamo, M., Kukkonen, M., Packalen, P., 2023. Assessing biodiversity using forest structure indicators based on airborne laser scanning data. Forest Ecology and Management 546, 121376. doi:10.1016/j.foreco.2023.121376.

Vincent, G., Antin, C., Laurans, M., Heurtebize, J., Durrieu, S., Lavalley, C., Dauzat, J., 2017. Mapping plant area index of tropical evergreen forest by airborne laser scanning. A cross-validation study using LAI2200 optical sensor. Remote Sensing of Environment 198, 254–266. doi:10.1016/j.rse.2017.05.034.

Wagner, W., Hollaus, M., Briese, C., Ducic, V., 2008. 3D vegetation mapping using small-footprint full-waveform airborne laser scanners. International Journal of Remote Sensing 29, 1433–1452. URL: https://www.tandfonline.com/doi/full/10.1080/01431160701736398, doi:10.1080/01431160701736398.

Wang, W., Li, Y., Huang, H., Hong, L., Du, S., Xie, L., Li, X., Guo, R., Tang, S., 2023. Branching the limits: Robust 3d tree reconstruction from incomplete laser point clouds. International Journal of Applied Earth Observation and Geoinformation 125, 103557. doi:10.1016/J.JAG.2023.103557. publisher: Elsevier.

Wang, Y., Fang, H., 2020. Estimation of LAI with the LiDAR technology: A review. Remote Sensing 12, 3457. URL: https://www.mdpi.com/2072-4292/12/20/3457, doi:10.3390/rs12203457.

Watt, P.J., Donoghue, D.N.M., 2005. Measuring forest structure with terrestrial laser scanning. International Journal of Remote Sensing 26, 1437–1446. URL: https://www.tandfonline.com/doi/full/10.1080/01431160512331337961, doi:10.1080/01431160512331337961.

Wei, S., Yin, T., Dissegna, M.A., Whittle, A.J., Ow, G.L.F., Yusof, M.L.M., Lauret, N., Gastellu-Etchegorry, J.P., 2020. An assessment study of three indirect methods for estimating leaf area density and leaf area index of individual trees. Agricultural and Forest Meteorology 292-293, 108101. URL: https://www.sciencedirect.com/science/article/pii/S0168192320302033, doi:https://doi.org/10.1016/j.agrformet.2020.108101.

Wilkes, P., Lau, A., Disney, M., Calders, K., Burt, A., Gonzalez de Tanago, J., Bartholomeus, H., Brede, B., Herold, M., 2017. Data acquisition considerations for Terrestrial Laser Scanning of forest plots. Remote Sensing of Environment 196, 140–153. doi:10.1016/j.rse.2017.04.030.

Williams, A., Barrus, S., Morley, R.K., Shirley, P., 2005. An efficient and robust ray-box intersection algorithm, in: ACM SIGGRAPH 2005 Courses on - SIGGRAPH '05, ACM Press, Los Angeles, California. p. 9. URL: http://portal.acm.org/citation.cfm?doid=1198555.1198748, doi:10.1145/1198555.1198748.

Winiwarter, L., Esmorís Pena, A.M., Weiser, H., Anders, K., Martínez Sánchez, J., Searle, M., Höfle, B., 2022. Virtual laser scanning with helios++: A novel take on ray tracing-based simulation of topographic full-waveform 3d laser scanning. Remote Sensing of Environment 269, 112772. URL: https://www.sciencedirect.com/science/article/pii/S0034425721004922, doi:https://doi.org/10.1016/j.rse.2021.112772.

Xu, H., Huai, Y., Zhao, X., Meng, Q., Nie, X., Li, B., Lu, H., 2025. SK-TreePCN: Skeleton-embedded transformer model for point cloud completion of individual trees from simulated to real data. Remote Sensing 17, 656. URL: https://www.mdpi.com/2072-4292/17/4/656, doi:10.3390/rs17040656. number: 4 Publisher: Multidisciplinary Digital Publishing Institute.

Yin, D., Wang, L., Lu, Y., Shi, C., 2024. Mangrove tree height growth monitoring from multi-temporal uav-lidar. Remote Sensing of Environment

303, 114002. URL: https://www.sciencedirect.com/science/article/pii/S0034425724000130, doi:https://doi.org/10.1016/j.rse.2024.114002.

Yrttimaa, T., Saarinen, N., Kankare, V., Viljanen, N., Hynynen, J., Huuskonen, S., Holopainen, M., Hyyppä, J., Honkavaara, E., Vastaranta, M., 2020. Multisensorial Close-Range Sensing Generates Benefits for Characterization of Managed Scots Pine (Pinus sylvestris L.) Stands. ISPRS International Journal of Geo-Information 9, 309. doi:10.3390/ijgi9050309.

Yun, T., Cao, L., An, F., Chen, B., Xue, L., Li, W., Pincebourde, S., Smith, M.J., Eichhorn, M.P., 2019. Simulation of multi-platform LiDAR for assessing total leaf area in tree crowns. Agricultural and Forest Meteorology 276-277, 107610. URL: https://linkinghub.elsevier.com/retrieve/pii/S0168192319302187, doi:10.1016/j.agrformet.2019.06.009.

Zellweger, F., De Frenne, P., Lenoir, J., Vangansbeke, P., Verheyen, K., Bernhardt-Römermann, M., Baeten, L., Hédl, R., Berki, I., Brunet, J., Van Calster, H., Chudomelová, M., Decocq, G., Dirnböck, T., Durak, T., Heinken, T., Jaroszewicz, B., Kopecký, M., Máliš, F., Macek, M., Marek, M., Naaf, T., Nagel, T.A., Ortmann-Ajkai, A., Petřík, P., Pielech, R., Reczyńska, K., Schmidt, W., Standovár, T., Świerkosz, K., Teleki, B., Vild, O., Wulf, M., Coomes, D., 2020. Forest microclimate dynamics drive plant responses to warming. Science in press, 772–775.

Zhang, T., Hu, C., Han, J., Sun, H., Wang, R., Jing, Z., 2025. TreegrowNet: a completion network for incomplete single tree point cloud from TLS. International Journal of Remote Sensing 46. URL: https://doi.org/10.1080/01431161.2024.2440134, doi:10.1080/01431161.2024.2440134. publisher: Taylor & Francis _eprint: https://doi.org/10.1080/01431161.2024.2440134.

Zhu, Y., Li, D., Fan, J., Zhang, H., Eichhorn, M.P., Wang, X., Yun, T., 2023. A reinterpretation of the gap fraction of tree crowns from the perspectives of computer graphics and porous media theory. Frontiers in Plant Science Volume 14 - 2023. URL: https://www.frontiersin.org/journals/plant-science/articles/10.3389/fpls.2023.1109443, doi:10.3389/fpls.2023.1109443.